Hurley, John Kevin

CHLOROPHYLL PHOTOCHEMISTRY IN LIPOSOMES: TRIPLET STATE QUENCHING AND ELECTRON TRANSFER TO QUINONE

The University of Arizona PH.D. 1982

CHLOROPHYLL PHOTOCHEMISTRY IN LIPOSOMES: TRIPLET STATE QUENCHING AND ELECTRON TRANSFER TO QUINONE

by

John Kevin Hurley

A Dissertation Submitted to the Faculty of the

DEPARTMENT OF CHEMISTRY

In Partial Fulfillment of the Requirements
For the Degree of

DOCTOR OF PHILOSOPHY

In the Graduate College

THE UNIVERSITY OF ARIZONA

1 9 8 2

THE UNIVERSITY OF ARIZONA
GRADUATE COLLEGE

As members of the Final Examination Committee, we certify that we have read the dissertation prepared by John Kevin Hurley

entitled Chlorophyll Photochemistry In Liposomes: Triplet State Quenching And Electron Transfer to Quinone

and recommend that it be accepted as fulfilling the dissertation requirement for the Degree of Doctor of Philosophy.

	March 31, 1982 Date
	March 31, 1982 Date
	March 31, 1982 Date
	March 31, 1982 Date
	March 31, 1982 Date

Final approval and acceptance of this dissertation is contingent upon the candidate's submission of the final copy of the dissertation to the Graduate College.

I hereby certify that I have read this dissertation prepared under my direction and recommend that it be accepted as fulfilling the dissertation requirement.

Dissertation Director	March 31, 1982 Date

STATEMENT BY AUTHOR

This dissertation has been submitted in partial fulfillment of requirements for an advanced degree at The University of Arizona and is deposited in the University Library to be made available to borrowers under rules of the Library.

Brief quotations from this dissertation are allowable without special permission, provided that accurate acknowledgment of source is made. Requests for permission for extended quotation from or reproduction of this manuscript in whole or in part may be granted by the head of the major department or the Dean of the Graduate College when in his judgment the proposed use of the material is in the interests of scholarship. In all other instances, however, permission must be obtained from the author.

SIGNED: 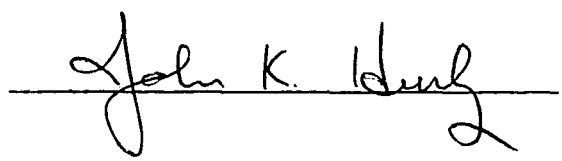

ACKNOWLEDGMENTS

I wish to express my deep and sincere gratitude to Dr. Gordon Tollin for his continued patience, guidance and understanding as a friend as well as a research director throughout the course of my graduate career. Special thanks are due Dr. Michael Cusanovich for his encouragement and for the use of his laboratory equipment and materials which I often had need of and to Dr. Michael Wells for help in the preparation of phosphatidylcholine. Patrick Kanda's invaluable help in the latter endeavor is likewise acknowledged as is the help of Malcolm Capel in various aspects of the work. Special thanks are also due Dr. Francesco Castelli who worked very closely on this project and contributed numerous helpful ideas and suggestions. I am also thankful to Dr. R. Clinton Fuller for originally getting me interested in the study of photosynthesis. I am also very thankful to the many wonderful friends of mine in Tucson whose encouragement and whose friendship and company through the good times and through the bad times helped me maintain my sanity. Special thanks are undeniably due my family for continually spurring me on to the finish and especially to my mother and father, Grace F. Hurley and John J. Hurley whose magnanimous sacrifices and encouragement allowed me to get started in this field.

TABLE OF CONTENTS

		Page
	LIST OF ILLUSTRATIONS	v
	LIST OF TABLES	vii
	ABSTRACT	viii
1.	INTRODUCTION	1
	Chlorophyll-Quinone Photochemistry in Solution	4
	General Properties of Liposomes	9
	Structural and Spectroscopic Properties of Chl-liposomes	12
	Chlorophyll Photochemistry in Liposomes	20
2.	EXPERIMENTAL	26
	Materials	26
	Instruments	26
	Procedures	28
	Sample Preparation	28
	Data Analysis	30
3.	RESULTS AND DISCUSSION	37
	Self Quenching of the Chlorophyll Triplet State	37
	Electron Transfer to Quinone	50
	Concluding Remarks	75
	APPENDIX A: LIST OF SYMBOLS AND ABBREVIATIONS	79
	SELECTED BIBLIOGRAPHY	81

LIST OF ILLUSTRATIONS

Figure		Page
1.	Visible absorption spectrum of Chl_t	5
2.	Visible absorption spectrum of $Chl^{+\cdot}$	6
3.	Absorption spectrum of $BQ^{-\cdot}$	7
4.	Diagrammatic representation of liposome structure	10
5.	Visible absorption spectrum of Chl in egg PC liposomes and in diethyl ether	13
6.	Scatchard plot of the binding of BQ to egg PC liposomes	35
7.	Difference spectrum of Chl_t	38
8.	First order plots of the decay of Chl_t	40
9.	Decay curves of Chl_t in liposomes at various Chl concentrations	42
10.	First order plots of the decay of Chl_t in liposomes at various Chl concentrations	43
11.	Concentration quenching curve of photo-excited Chl	45
12.	Stern-Volmer plot of Chl_t self-quenching in liposomes	48
13.	(a) Biphasic decay of Chl_t and $Chl^{+\cdot}$ in Chl-liposomes in the presence of BQ. (b) Decay at longer times	52
14.	Difference spectrum of Chl-liposomes in the presence of quinones	53
15.	$Chl^{+\cdot}$ and Chl_t yields as a function of UQ concentration	55
16.	Stern-Volmer plots of Chl_t quenching by BQ (o) and UQ (o)	56
17.	$Chl^{+\cdot}$ decays with quinone present	58
18.	Relative Chl_t and $Chl^{+\cdot}$ yields as a function of average number of Chl/liposomes	60

LIST OF ILLUSTRATIONS--Continued

Figure		Page
19.	Dependence of the slow component of the $Chl^{+\cdot}$ decay on the apparent BQ concentration	64
20.	Invariance of the decay rate of fast component of the $Chl^{+\cdot}$ decay as a function of Chl and UQ concentrations	65
21.	Hypothetical scheme for electron transfer between Chl and quinones in liposomes	66
22.	Concentration of $Chl^{+\cdot}$ produced as a function of quinone concentration	68
23.	Decay of $Chl^{+\cdot}$ in DPPC and DOPC liposomes	70
24.	Concentration of $Chl^{+\cdot}$ produced as a function of the fraction of Chl_t quenched $(1 - \tau/\tau_o)$	71

LIST OF TABLES

Table Page

1. Electron transfer to quinones in various lipid bilayers 57

2. Radical production and triplet quenching parameters indicating quinone-quinone electron transfer 73

ABSTRACT

Liposomes incorporating chlorophyll (Chl) have been used as a model system to study various aspects of photosynthesis (such as Chl photo-oxidation and acceptor reduction). Laser flash photolysis studies of this system have demonstrated that the Chl triplet state (Chl_t) can transfer an electron to acceptors such as quinones, resulting in the formation of the Chl cation radical ($Chl^{+\cdot}$) and the semiquinone anion radical ($Q^{-\cdot}$).

Quenching of Chl_t by quinones in liposomes is diffusion-controlled. The quenching rate is dependent upon bilayer viscosity. Chl_t lifetimes in the absence of quinones also reflect bilayer viscosity.

Radical decay occurs by reverse electron transfer. Although the decay is non-exponential, the decay rate is independent of laser intensity. This is presumably because radical pairs once formed do not become independent of one another and back react in a manner which can be likened to geminate recombination. The non-exponentiality is due to electron exchange between quinone molecules and the heterogeneity in the distribution of molecules among the vesicles. This electron exchange is also manifested in the radical formation process. At high quinone concentration the radical yield increases with quinone concentration in non-linear fashion with respect to the amount of triplet quenched. This positive cooperative effect is interpreted in terms of high quinone concentrations increasing the efficiency of radical production by

providing a pathway (via electron hopping) for removal of the electron from the site of initial electron transfer.

When ubiquinone is used, only a single fast decay is observed. However, when quinones which can partition between the aqueous and lipid phases are used, radical decay occurs via a fast and a slow process. This is interpreted in terms of electron transfers from $Q^{\cdot -}$ within the bilayer to Q at the bilayer-water interface which results in a stabilization of the electron transfer products and a slowly-decaying radical. The rate of this slow decay process is also quinone concentration dependent, which is a consequence of a facilitation of electron return to $Chl^{+\cdot}$ by Q molecules within the bilayer via an electron hopping mechanism. That such a mechanism is, in fact, operative in radical production is shown also by the observation of electron transfer from $UQ^{\cdot -}$ to BQ molecules.

CHAPTER 1

INTRODUCTION

Photosynthesis has long been a subject of extensive research by workers in diverse fields of the physical and biological sciences. Those involved in bioenergetics have studied this process with a hope of elucidating the mechanism of the primary event of photosynthesis, i.e., the electron transfer process which is initiated by the photoexcitation of chlorophyll (Chl) in the photosynthetic reaction center. The ultimate results of this light-induced electron transfer in green plants are the oxidation of water (resulting in O_2 production) and the fixation of CO_2 into carbohydrate, thereby storing a significant fraction of the absorbed electromagnetic energy in the form of chemical bond energy. The primary event of bacterial photosynthesis involves the oxidation of a dimeric form [1-4] of bacteriochlorophyll (BChl) which is situated in a specialized environment which renders it capable of functioning as the photoactive center. Concomitant with this is the reduction of the primary acceptor, bacteriopheophytin (BPhe, Mg^{+2}-free BChl) [5,6]. BPhe thereby serves as a mediator in the reduction of ubiquinone (UQ), a benzoquinone (BQ) derivative, in bacterial photosynthesis. In green plant photosynthesis two different photosystems are active which are generally referred to as photosystem I (PSI) and photosystem II (PSII). The photoactive Chl species in these two centers are referred to as P700 and P680, respectively. This particular designation refers to wavelengths at which

absorption changes are observed which correlate with the functioning of the two pigment systems. In PSI the primary electron acceptor appears to be a monomeric Chl molecule while in PSII an electron is transferred to plastoquinone (another BQ derivative) with pheophytin (Phe, Mg^{+2}-free Chl) acting as an intermediary electron acceptor, much like the bacterial system [7]. The primary electron transfer reactions, at least in the bacterial photosynthetic systems which are to date the best understood, proceed with virtually 100% efficiency in terms of quantum conversion into primary products [8]. The analagous reaction in PSI of green plants has been determined to be at least 75% efficient [9].

As a means of exploring the mechanism of the primary photochemical events, numerous analogs of these reactions involving Chl have been studied in model systems. Additionally, in view of the relatively high efficiency of photosynthetic systems, many workers are also currently attempting to simulate the photosynthetic electron transfer reaction in such model systems [10-13] with a view toward developing a practical photochemical cell utilizing Chl.

In attempts to understand the functioning of Chl in vivo, the one-electron photoreduction of quinones by Chl has been extensively studied in solution and the mechanism of this reaction is now quite well understood. As an extension of this solution work, these reactions are also being studied in heterogeneous systems such as Chl-containing liposomes (Chl-liposomes) and this aspect of Chl-quinone photochemistry is the subject of this dissertation. The latter system constitutes a more complex model system somewhat closer in structure to the in vivo photosynthetic system than are simple solutions and should lend further

insight into the functioning of Chl in photosynthesis. As will be described below, this particular model has the advantage of permitting compartmentalization of the processes involved in light absorption and electron transfer while at the same time can be conveniently studied by optical methods. For information concerning other model systems the interested reader should consult the available literature. For example, reports of investigations of electronic processes in planar lipid bilayers membranes (BLMs) were presented at the Symposium on Photoelectric Bilayer Membranes (June 1975) and the proceedings have been published [14] as has a more recent review [15]. For work involving micellar systems, the reader is directed to current reviews [16,17] and to several research papers [18-21], as well as to references contained therein. Still other model systems, such as Chl incorporated into polymer films [22], into polymeric particles [23,24], into mono- [25,26] and multi-layer arrays [27,28], some of which are deposited on electrode surfaces [29-33], into microemulsions [34-36], and into non-specific lipid and protein particles [37] are also noteworthy.

Since studies of the photochemical reduction of quinone by Chl-liposomes are an extension of work previously done in solution, the current state of knowledge regarding Chl-quinone photochemistry in solution will be briefly summarized. Liposome structure, the interaction of Chl with liposomes, and previously studied Chl-quinone photochemistry in liposomes will also be described before the material comprising the subject of this dissertation is presented.

Chlorophyll-Quinone Photochemistry in Solution

The photoreduction of quinones by Chl has been studied by NMR, EPR, and flash photolysis. The products of this reaction are the Chl cation radical ($Chl^{+\cdot}$) and the semiquinone anion radical ($Q^{-\cdot}$). These species are easily monitored spectroscopically since the spectra of $Chl^{+\cdot}$ [38] and $Q^{-\cdot}$ [39] are known as is the spectrum of the Chl triplet state (Chl_t) [40], the reactive excited state of Chl which gives rise to these species (see below). The spectra of Chl_t, $Chl^{+\cdot}$ and $Q^{-\cdot}$ are shown in Figures 1, 2 and 3, respectively. Most of this work has been carried out in ethanol and other organic solvents. The role of photo-excited Chl in these reactions was shown by determining the yield of electron transfer products as a function of the wavelength of exciting light [41]. The action spectrum coincided with the absorption spectrum of Chl. It has been further shown that in solution, electron transfer to quinone occurs only from Chl_t [42,43]. This was initially implied by observing a decrease in yield of electron transfer products in the presence of Chl_t quenchers such as napthacene [44], β-carotene and O_2 [45]. More recently, laser flash photolysis has allowed a more direct confirmation of the precursor role of Chl_t in quinone photoreduction [42]. In these studies the rise of $Q^{-\cdot}$ was shown to parallel the decay of Chl_t. The effect of temperature and of quinone potential were also examined while in a later investigation [46] the effect of viscosity and dielectric properties of the solvent were studied. The results of this work are summarized below.

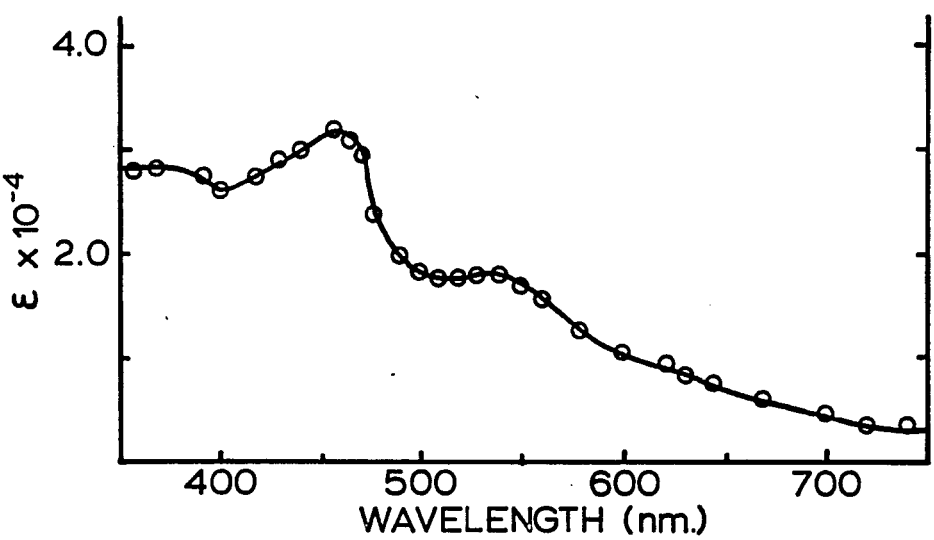

Figure 1. Visible absorption spectrum of Chl_t.

This spectrum is from reference 40. The solvent is pyridine.

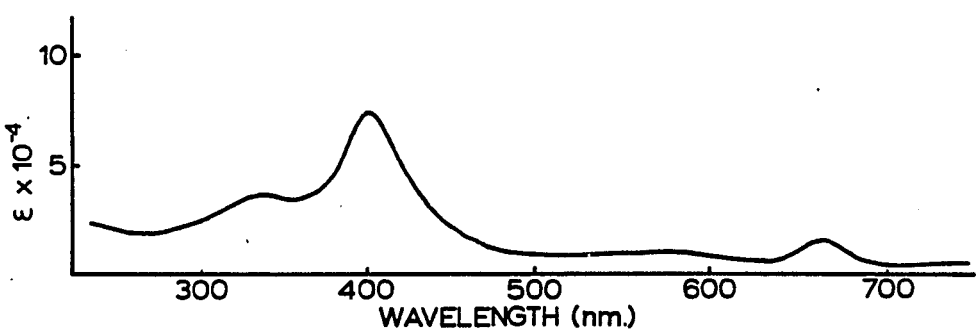

Figure 2. Visible absorption spectrum of Chl^{+}.

This spectrum is from reference 38. The solvent is dichloromethane.

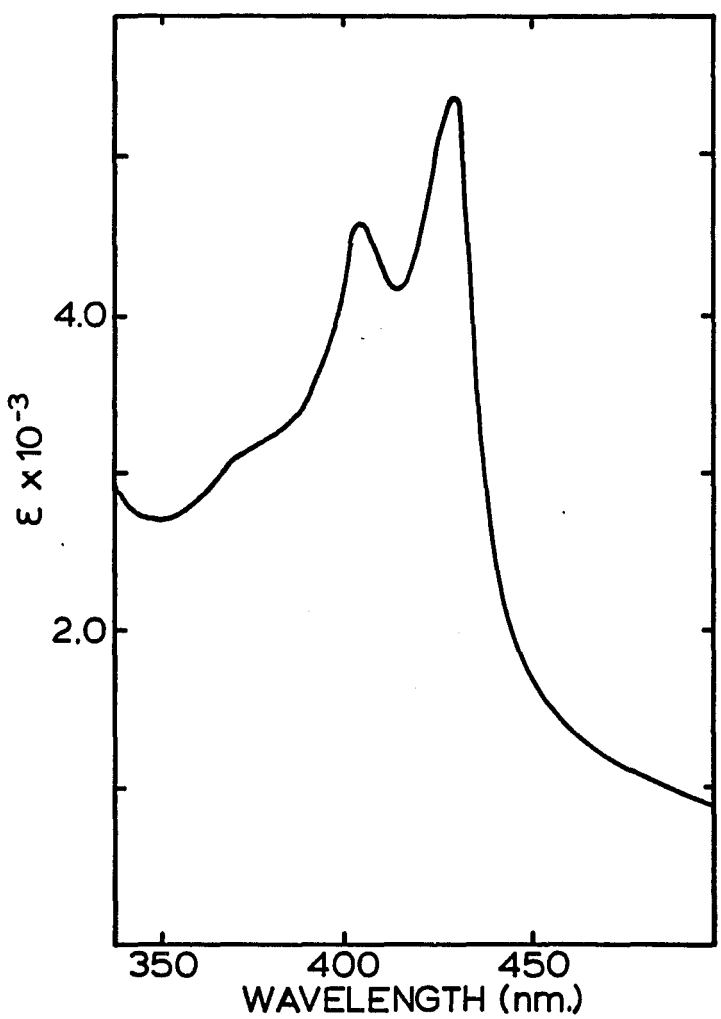

Figure 3. Absorption spectrum of $BQ^{\cdot -}$.

This spectrum is from reference 39. This is an aqueous solution.

Electron transfer from Chl_t to BQ occurs with about 70% efficiency in terms of conversion of Chl_t to $Chl^{+\cdot}$. Approximately 90% of the separated radical products decay by reverse electron transfer with a second order rate constant of $2 \times 10^9\ M^{-1}s^{-1}$ [42]. The other 10% of $Chl^{+\cdot}$ presumably reacts with solvent to regenerate Chl [34,47], thereby leaving the remaining $Q^{-\cdot}$ to decay by disproportionation [48,49]. A mechanism consistent with these results and those summarized below is as follows:

$$Chl + h\nu \longrightarrow Chl_s$$

$$Chl_s + Q \longrightarrow (Chl^{+\cdot} \ldots Q^{-\cdot})_s \longrightarrow Chl + Q$$

$$Chl_s \longrightarrow Chl_t$$

$$Chl_t + Q \xrightarrow{k_q} (Chl^{+\cdot} \ldots Q^{-\cdot})_t \longrightarrow Chl^{+\cdot} + Q^{-\cdot}$$

$$(Chl^{+\cdot} \ldots Q^{-\cdot})_t \longrightarrow Chl + Q$$

$$Chl^{+\cdot} + \text{solvent} \longrightarrow Chl + \text{oxidized solvent}$$

$$2Q^{-\cdot} + 2H^{+} \longrightarrow Q + H_2Q$$

Radical yield shows a linear dependence on quinone potential as is also true of the Chl_t quenching constant (k_q). Due to the increased facility of electron transfer from Chl_t and the increased tightness with which the electron is held in the semiquinone radical (allowing more radicals to separate before reverse electron transfer has occurred) an increase in radical yield is obtained at higher quinone potential. The quenching of Chl_t is also dependent on solvent viscosity. Thus, in highly viscous media quenching is slowed due to decreased diffusion. The reverse electron transfer is independent of quinone potential but does show a

temperature effect which appears to correlate with changes in solvent viscosity. Room temperature measurements in solvents of different viscosities [46] confirm this latter supposition. In addition, radical yields show a linear dependence on dielectric constant [46] above a certain threshold value (10-12). This is a consequence of a lowered electrostatic attraction of the radicals in the complex at higher dielectric constant thereby allowing facilitated separation of these species. Thus, the physical properties of the medium in which these reactions occur can have a profound influence on their efficiencies.

General Properties of Liposomes

Liposomes (sometimes called lipid bilayer vesicles) are quasi-spherical multimolecular assemblies in which a lipid bilayer (or several concentric bilayers) separates an inner aqueous compartment from the bulk water phase. The structure of the liposome is such that the polar head groups of the lipids are exposed to the aqueous phase on both faces of the bilayer, while the hydrocarbon chains of the lipids dissolve within themselves comprising the inner core of the bilayer (Fig. 4). Various preparation methods yield vesicles ranging from 250 Å - 2500 Å in diameter. Generally, naturally-occurring membrane lipids, especially the phospholipids (i.e. phosphatidylcholine, phosphatidylethanolamine, etc.), have been employed, as have their synthetic analogs, but non-physiological amphiphiles [50-52] can also form liposomes. Single chain surfactants such as the commonly used detergents generally form micelles [53]. The vesicles can be classified into two general categories: unilamellar (single bilayer per liposome) or multilamellar (several

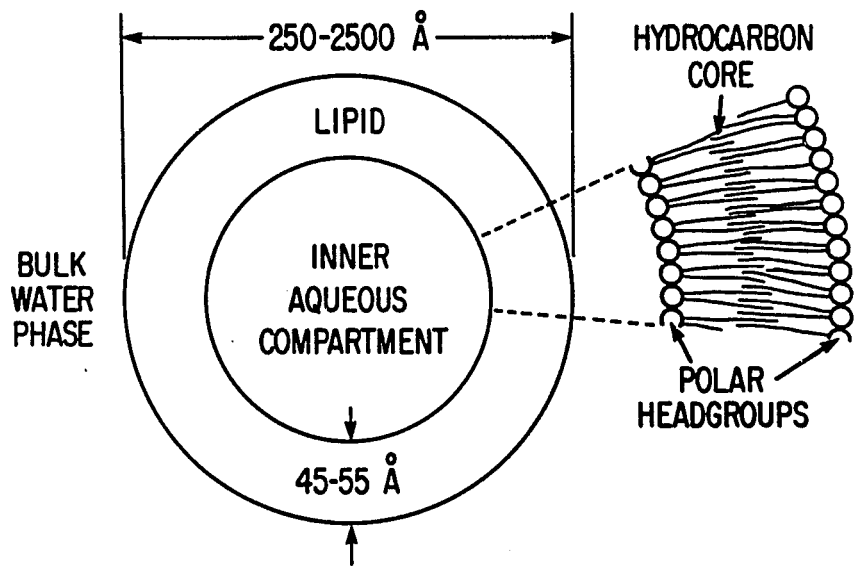

Figure 4. Diagrammatic representation of liposome structure.

concentric bilayers per liposome). The first liposome structures (multilamellar) were reported by Bangham et al. [54]. The formation of unilamellar vesicles by prolonged sonication of lipid dispersions followed by gel filtration was later reported by Huang [55]. Since then several other methods for preparing unilamellar vesicles have been reported including injection [56-58] of organic solutions into aqueous buffer, cholate dialysis [59], and ultracentrifugation [60]. Various physical parameters can be manipulated in liposomes including head group structure (which involves membrane surface charge), hydrocarbon chain length and degree of unsaturation. The latter two parameters affect the relative fluidity of the bilayer. This property has been extensively studied and it is now well known that the lipid phase can exist in either a liquid or a gel-like state depending upon the temperature and lipid composition. A gel-liquid phase transition occurs at a characteristic temperature (T_c) caused by a "melting" of the fatty acyl side chains of the lipids. Below T_c, the lipid bilayer is relatively rigid, whereas above T_c it is relatively fluid. The actual temperature of this phase transition depends upon the structure of the lipid. Thus, for instance, the transition temperature for dimyristoyl phosphatidylcholine (DMPC), dipalmitoyl phosphatidylcholine (DPPC) and distearoyl phosphatidylcholine (DSPC) are 23°, 41° and 55°, respectively. The increasing T_c values are due to an additional two methylene groups in each hydrocarbon chain of the lipid which increases the extent of interaction between the chains. Dioleoyl phosphatidylcholine (DOPC) shows a transition at -22°. This decrease in T_c, relative to that of DSPC, is due to the introduction of a double bond which disorders the

hydrocarbon core thereby disturbing the extensive intermolecular interactions which occur in the totally saturated lipid. For more information on these and other characteristics of liposomes the interested reader is directed to a recent review [61].

Structural and Spectroscopic Properties of Chl-liposomes

Many hydrophobic and amphipathic molecules can be solubilized by liposomes and their position within the bilayer (which is not always easy to evaluate) depends upon (among other things) their relative degree of hydrophilicity vs. hydrophobicity. Chl is one such molecule which, not long after the first literature reports of liposome preparation, was shown to be incorporated into vesicles if present during their formation [62]. Chl is stabilized toward photooxidation in the presence of phospholipids in homogeneous solution [63] or in liposomes [64]. It was later demonstrated that Chl incorporation had little effect on the liposome structure [65-67] although the average Stokes radius was shown to be reduced by approximately 10 Å in the presence of Chl and the magnitude of this change was independent of Chl concentration [65]. This may reflect a change in lipid packing density. In the earlier studies, glycolipids as well as phospholipids were found to solubilize Chl into the bilayer phase [62], and visible absorption spectral properties were reported. A red shift of approximately 10 nm was observed for the long wavelength absorption band, as compared to its position in ether solution (Fig. 5). Such a spectral change is consistent with the macrocylic ring of Chl being in a polar environment, i.e. close to the charged head group region and possibly slightly

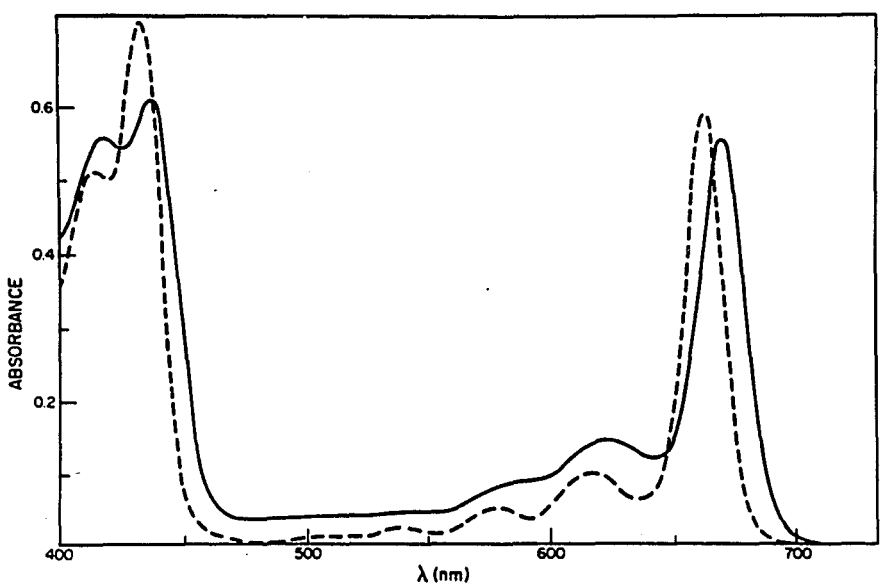

Figure 5. Visible absorption spectrum of Chl in egg PC liposomes and in diethyl ether.

The solid line represents the Chl-liposome spectrum whereas the broken line represents the spectrum in diethyl ether.

exposed to the aqueous environment. This shift was later confirmed [68] and has been observed in virtually all further studies. It was also noted that a depression of the 438 nm absorption band in the Soret region and an enhancement of its blue satellite occurred. This was attributed to association (the nature of this association was not specified by the authors) with phosphatidylcholine (PC), since the same effect had been observed with PC and Chl in chloroform solution where vesicle formation did not occur. A recent study of Chl-liposomes has shown that Chl absorbance is a linear function of Chl:PC mole ratio and of the PC concentration at a given Chl:PC ratio, indicating that the Chl is ideally mixed in the membrane [66].

There is considerable further evidence which indicates that the macrocylic ring of Chl is situated in or near the polar head group region of the liposome. In one study [69], perturbations of the EPR signals due to nitroxide spin labels located at various positions along the fatty acid side chains within liposomes were monitored upon incorporation of phytol, propionic acid phytol ester or Chl into the liposome. The results were consistent with the aforementioned positioning of Chl. As additional confirmation, these authors also found that the rates of photodestruction of the spin labels by reaction with Chl were fastest for those nitroxide groups closest to the head group region. Paramagnetic quenching experiments of Chl fluorescence are also in accord with these results [70]. In these studies, again using spin-labelled fatty acids with various positions of the label along the fatty acid chain, it was shown that the quenching of Chl

fluorescence became increasingly more efficient as the spin label approached the head group region of the liposome. In still another type of study, it has been shown that the macrocylic ring is accessible from the aqueous phase, as demonstrated by the fact that $K_2S_2O_8$, a non-permeating oxidizing agent, destroys at least half of the Chl when added to a Chl-liposome suspension [66,71]. A similar result had previously been obtained in BLMs [72].

The angle of tilt between the plane of the macrocylic ring of Chl and the plane of the bilayer has also been investigated. Polarized absorption spectroscopy in BLMs has led to the conclusion that the two planes make a 48° angle with respect to one another [73], thereby substantiating an earlier contention by the same authors that the macrocylic rings were at least partially oriented [74]. Linear dichroism studies, also using BLMs, were in good agreement with this value, yielding angles of between 44° and 49° in cases in which three different phospholipids were used [75]. An investigation employing photovoltage spectroscopy was consistent with an angle of 45° [76], while another polarization spectroscopy study [77] yielded a 55° angle. Experiments utilizing low angle x-ray diffraction and absorption polarization spectroscopy on hydrated multilayers, and nuclear magnetic resonance spectroscopy on unilamellar liposomes [78], have indicated an angle of 54°. This same study also showed that the phytol chain penetrates into the hydrocarbon core of the bilayer in an extended conformation. In agreement with the spectroscopic results are calorimetric experiments which indicate that incorporating Chl into liposomes abolishes the

pretransition, due to interactions of the macrocylic ring with the polar head groups, and at the same time broadens the main transition, due to the positioning of the phytol side chains of Chl among the hydrocarbon chains of the lipids [79]. Finally, another set of experiments [80,81], which demonstrated slight changes in Chl absorption spectral properties upon incorporation of valinomycin into the liposome structure, was interpreted in terms of a solvatochromic effect brought about by changes in the orientation of the head group. This is again consistent with the aforementioned conclusions regarding the positioning of the Chl macrocycle with respect to the aqueous-lipid interface.

A variety of fluorescence studies in Chl-liposomes have been performed. Early experiments demonstrated an increase in fluorescence yield of Chl in liposomes comprised of saturated lipids as the temperature was taken above the gel-liquid phase transition temperature (T_c). Since Chl aggregates are known to fluoresce weakly if at all [82-88], this was taken to mean that Chl existed in an aggregated form below T_c and in a monomeric (fluorescent) form above T_c [89]. No absorption spectral changes which could be correlated with aggregation were observed in this study (at 1 mole % to 25 mole % Chl). In a later, more detailed investigation [79,90], similar fluorescent changes were seen at T_c, although in this case it was reported that above T_c the absorption bandwidth increased at increasing Chl concentrations (above 1.25 mole % Chl) due to the appearance of a shoulder at 685 nm [79] which was taken as an indication of aggregation. It was also shown that only one fluorescent form of Chl was present in this system. Another report demonstrated that as liposomes were cooled below T_c,

there was a red shift of the long wavelength absorption band of Chl b [91], although no noticeable shift was observed in an analogous experiment employing Chl a. The spectral shift of Chl b was less pronounced in DMPC than in DPPC-liposomes. A more recent study is in agreement with fluorescence intensity changes at T_c, but no changes were observed in the absorption bandwidth, either above or below T_c, up to 10 mole % Chl [92]. Absorption wavelength characteristics also showed no temperature dependence as was true of the position of the fluorescence band. It was only the fluorescence intensity that showed a temperature effect, except at low Chl:lipid ratios (0.33 mole % Chl). Here, no change in fluorescence intensity was seen in going through T_c presumably because Chl is at a concentration below its solubility limit, allowing dispersed monomeric Chl, even in the crystalline state of the membrane. A similar study was in agreement with the disappearance of the sharp change in fluorescence at T_c at about 0.33 mole % Chl [93]. In other experiments Chl aggregates were observed directly by the presence of a long wavelength absorption band at 750 nm [94,95]. As will be discussed in the next section, these aggregates were shown to affect the quantum yield of transmembrane electron transfer. Thus it appears that Chl is present in a highly aggregated state below T_c, except at very low Chl:PC mole ratios, and that it is highly dispersed above T_c, although there is some spectroscopic evidence in favor of minimal aggregation when the lipid is in the fluid state. Although the latter has not been borne out in all studies, it should be pointed out that some properties of Chl-liposomes are dependent on their method of preparation [67].

Fluorescence intensity decreases have been observed in Chl-liposomes as the temperature was increased from 25°-40° (above T_c) [67]. This was attributed to increased diffusion-controlled self-quenching. A fairly detailed analysis of this phenomenon has been reported [96]. The main conclusions were that no aggregation was occurring and that fluorescence quenching was due to multistep resonance energy transfer among Chl molecules which is culminated by transfer to an energy trap. The trapping center was suggested to be a statistical pair consisting of any two Chl molecules separated by less than 10Å. The Chl fluorescence lifetime was 5.7 ns in dilute suspensions. The concentration dependence of fluorescence quenching was shown to be somewhat dependent on the mechanism of vesicle preparation as well as on the structure of the lipid. Thus, higher Chl concentrations were needed to half-quench the fluorescence in vesicles prepared by shaking (which yields large multilamellar vesicles) as compared to those prepared by sonication (which yields small unilamellar vesicles). Higher concentrations were also needed in vesicles composed of galactolipids as opposed to egg PC. As pointed out by the authors, the former observation may be due to a larger radius of curvature for the bilayer in the sonicated preparation, forcing Chl molecules closer together on the inside bilayer and thereby increasing the concentration of statistical pair traps. The latter observation regarding lipid structure was explained as being due to the fact that the galactolipids, being more bulky and having more possibilities for hydrogen bonding to Chl carbonyl groups or for coordination with the magnesium, are more efficient at keeping Chl molecules further apart than the trap forming

distance. A similar role for β-carotene in maintaining this distance, at least in liposomes, has also been demonstrated [97]. The result with the galactolipids is interesting in that these are known to be the most abundant lipid type found in photosynthetic membranes. The absence of aggregates was inferred from the lack of any change in absorption or emission spectral properties, as well as from the fact that the fluorescence yield and lifetime curves were coincident. Aggregate formation would cause a decrease in yield while no change in lifetime would be expected.

EPR experiments in which Chl (in liposomes) was photooxidized in the presence of oxidants such as $K_3Fe(CN)_6$, $SmCl_3$ or $EuCl_3$ are also consistent with a monomeric state of Chl in the liposomes under the conditions used (up to 10 mole % Chl). The EPR signal due to $Chl^{+\cdot}$ had a g value of 2.0026±0.0003 and a line width of 9.0±0.5 G [98,99]. These values are charcteristic of monomeric $Chl^{+\cdot}$ [100]. These same authors also demonstrated the absence of Chl-Chl interactions by circular dichroism measurements which yielded spectra essentially identical with what is observed for monomeric Chl in solution. Another EPR study [101], utilizing iodine as well as a number of organic oxidants, gave EPR spectral parameters which are in agreement with the study mentioned above. These experiments will be discussed in more detail in the next section.

Chlorophyll Photochemistry in Liposomes

Several previous studies on Chl-photosensitized electron transfer reactions in liposomes have been performed and these will be described in this section. Early work demonstrated the direct photoreduction of cytochrome c (cyt c) by Chl-liposomes [62]. However, in a later investigation [84], it was found necessary to add hydrogen donors such as trimethylhydroquinone in order to obtain cyt c reduction. This was true even when a negative charge was present on the liposome surface (by incorporation of phosphatidic acid), which would presumably increase the extent of binding of the positively charged cyt c. The latter authors suggested the possible presence of endogenous donors to explain the results obtained in the earlier study. In this same series of experiments, the photocatalytic reduction of cyt c was found to be negligible below T_c when Chl b-DPPC liposomes were used. However, when DMPC liposomes were employed, or when Chl a (Chl b differs from Chl a by having a formyl group in place of the methyl group on ring II of the macrocyclic ring) was the sensitizer in either lipid, similar but much less striking changes were seen at T_c. This correlates with similar smaller spectral shifts of Chl a in these systems as mentioned above. The lack of catalytic reduction of cyt c in the Chl b-DPPC liposomes below T_c was thought to be due to either a reduced permeability of the hydroquinone/quinone or to a decrease in the production of reactive Chl excited state. Since no direct measurements of either parameter were made, the mechanism must remain open.

Several EPR studies on photoinduced electron transfer reactions in Chl-liposomes have been reported. In one such investigation [98,99],

it was shown that when inorganic acceptors such as $K_3Fe(CN)_6$, $SmCl_3$ or $EuCl_3$ were used, a photoinduced EPR signal due to $Chl^{+\cdot}$ was observed. Temperature dependence studies showed that from liquid helium temperature up to about -100°C, the light-induced signal did not decay for several hours, and a measurable decay became evident only above -100°C. The decays of the radical signals at low temperature were qualitatively similar with $SmCl_3$ or $K_3Fe(CN)_6$ as oxidants, but at room temperature the decays were quite different. With $K_3Fe(CN)_6$, the signal decayed faster than the time constant of the instrument (1s) when the light was turned off, whereas with $SmCl_3$ the decay was biphasic with a large portion of the signal taking minutes to decay. This suggested that part of the reduced species (Sm^{+2}) was probably reacting with some other component of the system, thereby leaving a portion of the cation radical to react in a slow process which was different from the reverse electron transfer reaction. In this regard it was noted that H_2 gas was produced in the case of $SmCl_3$, although this was a rather irreproducible phenomenon. When ubiquinone (UQ) or p-benzoquinone (BQ) were used as acceptors, no EPR signal due to either $Chl^{+\cdot}$ or to reduced quinone could be detected, although the possibility was raised that perhaps electron transfer was occurring but that the reverse electron transfer reaction was so fast that it precluded the observation of $Chl^{+\cdot}$.

In still another EPR study [101], $K_3Fe(CN)_6$ was found to be incapable of serving as an electron acceptor (in contrast to the aforementioned work), whereas Fe^{+3} pyrophosphate and methyl viologen, when used as acceptors, allowed the observation of an EPR signal attributable to $Chl^{+\cdot}$. Like $K_3Fe(CN)_6$, cyt c, flavin mononucleotide and nicotinamide

adenine dinucleotide were inactive. With BQ, 2-hydroxynaphthoquinone and anthraquinone-2-sulfonic acid, only EPR signals due to the semiquinone radicals could be observed upon illumination. No signal could be observed when UQ was used (as in the aforementioned study), as was also true of 2,5-dimethyl-p-benzoquinone. If N,N,N',N'-tetramethyl-p-phenylenediamine (TMPD) was present as an electron donor in the UQ/Chl-liposome system, an EPR signal due to $TMPD^{+}$ was seen upon illumination, and the formation of this signal was dependent on the presence of both Chl and UQ, indicating that Chl was photosensitizing the electron transfer from TMPD to UQ. An important point made by the authors is that the different behavior of various acceptors is in large part determined by their polarity, i.e., this property as well as others such as redox potential must be carefully weighed when choosing acceptors or interpreting results. It is also important to emphasize that negative steady-state experiments do not necessarily prove that electron transfer is absent, since rapid radical decay rates can lead to the same result.

Photosensitized charge transport across liposome membranes has also been studied. In one investigation [94], it was demonstrated that, if a redox gradient existed across the bilayer membrane, photoinduced reduction of Fe^{+3} present inside the vesicle by ascorbate outside could take place in liposomes which contained both Chl and β-carotene. The presence of both of these pigments was required. The quantum efficiency of this process (defined as the number of electrons transported divided by the number of photons absorbed) was determined to be 0.075. These preparations contained Chl aggregates as evidenced by an absorption

band at 750 nm. Since raising the temperature or adding pyridine destroyed this aggregation at the same time that the quantum efficiency was decreased by more than 75%, it was concluded that Chl aggregates were at least partially responsible for the relatively high efficiency observed for this system.

In another series of experiments [102], the reduction of Cu (II) present in the outer aqueous phase by ascorbate present within the vesicle was followed by EPR. That this reduction was not due to leakage of the ascorbate was ascertained by adding this substance to the outer solution. Under these conditions there was immediate and virtually quantitative reduction of Cu (II) irrespective of illumination. Also, there was a negligible dark signal in the situation where the Cu (II) and the ascorbate were compartmentalized. It was shown that the action spectrum for Cu (II) reduction agreed with the absorption spectrum of Chl. There was some irreversible bleaching of the Chl absorption, but the amount of bleaching was negligible compared to the amount of Cu (II) reduced. Contrary to the results of experiments described above, it was shown that reduction rates were not changed significantly if β-carotene was also incorporated into the liposomes. The reasons for this apparent discrepancy are not clear.

When $K_3Fe(CN)_6$ was used as acceptor in place of Cu (II), these same authors [103] demonstrated that addition of a proton carrier, such as carbonylcyanide-m-chlorophenylhydrazone (CCCP), greatly facilitated the photoinduced electron transfer across the liposome membrane. Not only were the initial reduction rates enhanced by CCCP addition, but also the amount of ferricyanide ultimately reduced was increased in the

presence of the uncoupler. Both of these parameters were shown to increase as a function of CCCP concentration until at higher concentrations saturation occurred. The fact that the amount of ferricyanide reduced was much greater than the amount of CCCP added demonstrated that the observed results were not due to a direct interaction of CCCP with $Fe(CN)_6^{-3}$. Again, the action spectrum coincided with the absorption spectrum of Chl. It was suggested that the enhancement effect of CCCP was due to its proton transport function, which would alleviate charge unbalance caused by the transmembrane electron transfer reaction. In this regard it was also shown (by following pH changes) that the hydrogen ion concentration did indeed increase in the extraliposomal phase, and that this light-induced pH change was dependent upon the presence of CCCP. EPR experiments showed that there was a photoinduced formation of $Chl^{+\cdot}$ during the course of the experiments just described.

Recent experiments utilizing oxygen uptake as a measure of transmembrane electron transfer [95] suggest that Chl can sensitize the ascorbate reduction of 2,6-dichlorophenol indophenol but not of methyl viologen (MV^{+2}).

Light-induced O_2 production in liposome preparations has been reported [104]. In this study, extracted chloroplast pigments including Chl a, Chl b, β-carotene and xanthophyll were incorporated into egg PC vesicles. Illumination of such a suspension with $K_3Fe(CN)_6$ present in the sequestered aqueous phase resulted in O_2 production, a characteristic of photosystems II in green plant photosynthesis. Although the yields were rather small the rate of O_2 production was approximately

proportional to the light intensity and the action spectrum was similar to the absorption spectrum of Chl. In the absence of $K_3Fe(CN)_6$, O_2 production was negligible. An attempt to repeat this experiment proved unsuccessful although O_2 was produced by thylakoid membrane fragments which had been fused with liposomes [105].

Thus, it is apparent that Chl-liposomes provide a viable biomimetic model system for studying Chl-sensitized photoreactions of green plant photosynthesis. The research described herein involves the study of Chl excited state quenching and electron transfer to quinone in such vesicles. A mechanism for radical formation and decay which is consistent with the data will be presented.

CHAPTER 2

EXPERIMENTAL

Materials

Chl was extracted from fresh spinach leaves and purified according to Strain and Svec [106]. Chromatographically pure egg phosphatidyl choline (egg PC) was obtained and purified according to the method of Wells and Hanahan [107], with the additional step of deionization [108] of the PC using Bio Rex 70 and Ag3-X4A ion exchange resins (Bio-Rad Laboratories). Dioleoyl-L-α-phosphatidylcholine (DOPC) and dipalmitoyl-L-α-phosphatidylcholine (DPPC) were purchased from Sigma Chemical Co. and were used without further purification. p-Benzoquinone (Eastman Organic Chemicals) was purified by vacuum sublimation (5x). Ubiquinone-30 (Sigma Chemical Co.) and 2,6-di-t-butyl-p-benzoquinone (Aldrich) were used without further purification. Duroquinone (Aldrich) was recrystallized from ethanol. Sepharose 4B was from Pharmacia Fine Chemicals. Deuterium oxide was purchased from Sigma Chemical Co. (99.8 mole % D_2O) and from Bio-Rad Laboratories (99.9 mole % D_2O). Ultrafiltration membranes (Diaflo UM10) and a Model 10-PA ultrafiltration device were from Amicon Corporation. All solvents and buffers were AR grade.

Instruments

Routine absorption spectra were obtained using a Coleman Model 124 Hitachi double-beam spectrophotometer, a Cary Model 118 or a Perkin Elmer Model 552 UV-VIS spectrophotometer. Fluorescence measurements

were made with instrumentation assembled in this laboratory and described previously [109]. Excitation was provided by an OSRAM high pressure xenon lamp. The output of this lamp was passed through a Bausch and Lomb 600 groove/mm grating monochromater. The exciting light was mechanically chopped at 240 Hz. Fluorescence emission was detected at right angles to the excitation beam utilizing another Bausch and Lomb 600 groove/mm grating monochromater, a quartz window photomultiplier and an EMC Model RJB lock-in amplifier.

The laser flash photolysis apparatus has also been described previously [42,110]. This apparatus utilized a pulsed nitrogen laser (National Research Group, Madison, WI) which was used to pump a dye laser consisting of a solution of Rhodamine 6G and cresyl violet (1 mM each in ethanol). The dye was contained in a 4 cm pathlength rectangular cuvette. This provided a 10 ns pulse at 655-660 nm. The monitoring beam which made an angle of approximately 10° with the excitation beam was provided by a quartz-iodine projection lamp which was focused through a Bausch and Lomb 1350 groove/mm grating monochromater before passing through a 1 cm^2 sample cell. The beam then passed through a 0.5 mm aperature and was focused onto an RCA 4462 photomultiplier tube (S-20 response). In the earliest experiments the flash-induced photo-response was measured using a Biomation Model 805 waveform recorder (0.2 μs per point time resolution). This was later replaced with a Biomation Model 8100 which has a better time resolution (10 ns per point). Signal averaging was accomplished using a Fabritek Model 1074 signal averager.

For the binding experiments involving centrifugation a Beckman L8 55 Ultracentrifuge and Ti 65 rotor were used.

Procedures

Sample Preparation

Liposomes were prepared by two different methods. One of these consisted of combining appropriate aliquots of PC (84 μmole - 0.1 mole) dissolved in methanol and Chl (7.2 μmole) dissolved in ethanol in a stainless steel cell (Heat Systems Ultrasonics). The organic solvents were then evaporated with a stream of nitrogen. When dry, 5 ml of 10 mM phosphate buffer (pH 7.0) was added and mixed on a Vortex mixer to achieve a homogenous dispersion. The suspension was bubbled with nitrogen for approximately 5 minutes and then sonicated in an ice bath under a nitrogen atmosphere for thirty minutes using a model S125 Branson Sonifier at power level 5. Samples were subsequently centrifuged at 20,000xg for 30 minutes to remove titanium particles. The second method utilized for liposome preparation [56] involved injecting an ethanolic solution of Chl and PC (20-40 μmoles/ml) into rapidly stirring phosphate buffer (pH 7.0). The volume injected was such that the final ethanol concentration was 5-7% (v/v). For preparation of DPPC liposomes, the buffer was heated to above the phase transition temperature of the lipid before injection. This resulted in no noticeable degradation of the Chl as judged by its visible absorption spectrum. Both preparative methods gave identical results with respect to the photochemistry discussed herein. In both cases, the entire sample preparation procedure was carried out under minimal light.

Enough Chl was added in each experiment to give a final absorbance (at 667 nm) of 0.5. The extinction coefficient used for

ethanolic Chl solutions was 6.9×10^4 [111]. The concentration of Chl within the liposome was altered by changing the amoung of lipid. Chl concentrations (M) within the liposome (also given as number of Chl molecules per liposome) were estimated assuming a homogeneous population of unilamellar liposomes and using the various size and weight parameters known for such liposomes [112]. Gel filtration using Sepharose 4B [55] indicated that at least 80% of the liposomes in our preparations were of the small unilamellar variety. Samples for photolysis were bubbled (5 min) and sealed under nitrogen. Samples for fluorescence measurements were not deoxygenated. The effect of O_2 in solution at atmospheric pressure on the very short-lived (compared to that of Chl_t) fluorescence lifetime of Chl is minimal and therefore deoxygenation of these samples was not deemed necessary. They were, however, diluted to an optical density of 0.1 to minimize self-absorption and light scattering. The latter was not a significant problem except at the highest lipid concentration and could be easily corrected for by adjusting the baseline.

For experiments with benzoquinone (BQ), this compound was added following liposome preparation. In the case of ubiquinone (UQ), duroquinone (DQ) and 2,6-di-t-butyl-p-benzoquinone (DTBQ), the quinone was present in the injected ehtanol solution along with the Chl and phospholipid.

DQ, DTBQ and UQ concentrations within the liposome were estimated by calculation as described above for Chl, assuming that all of the material was bound to the liposome. Because of the high degree

of water insolubility of these compounds, this is a good approximation. All concentrations specified as apparent refer to those which would result from uniform dispersion of the material throughout the total volume of the solution. The appreciable water solubility of BQ required an estimation of the extent of its partitioning between the vesicle and aqueous phases. This will be described below.

Data Analysis

The data obtained in the flash photolysis experiments consist of decay curves such as the ones shown in Figures 9 and 17. This is essentially a plot of voltage (ordinate) vs time (abscissa) and this voltage change can be correlated with optical density (OD or absorbance) changes as described below.

The output voltage from the photomultiplier tube (PMT) is proportional to the intensity of light impinging upon the photocathode. The baseline (initial flat portion of each trace prior to the flash-generated deflection) represents a voltage which is due to the monitoring beam traversing the sample cell and falling on the PMT when no transient is present. The light intensity transmitted by the sample cell when no transient is present, I_o, is proportional to the voltage change, V_o, (light off to light on) due to the monitoring beam intensity. Upon flash excitation of the sample, the light-generated transient species which are produced generally absorb more or less light relative to the species present in the sample cell prior to flash excitation and this results in a change in voltage output from the PMT. The intensity of light transmitted by the sample cell, I_t, at time, t, after the

flash (transient present) is proportional to the voltage output from the PMT, V_t (again relative to any voltage observed with the monitoring beam off) at time, t. The optical density, OD_t, at any time, t, is equal to log I_o/I_t which, for the reasons just discussed, is equal to log V_o/V_t. This OD_t is actually a change in OD (relative to the time immediately prior to flash excitation, i.e. no transient present) and shall be referred to as such (ΔOD_t) here. Thus

$$\Delta OD_t = \log V_o/V_t$$

This can be represented as shown here

$$\Delta OD_t = OD_T - OD_G$$

$$\Delta OD_t = \varepsilon_t b[Chl_t] - \varepsilon_g b[Chl_g]$$

where OD_T is the OD due to triplet being observed and OD_G is that due to ground state Chl which was depleted and ultimately (unless it returned to the ground state) gave rise to triplet. Since OD_G represents the ground state depletion it also is actually a change in the OD of the ground state brought about by the flash. The second equation shows these quantities in terms of Beer's Law where ε_t and ε_g are the extinction coefficients of the triplet and ground state respectively and $[Chl_t]$ and $[Chl_g]$ are their concentrations. Since the concentration of triplet absorbing is equal to the concentration of ground state depleted in order to form the concentration of triplet being observed at that particular time these two concentrations are essentially equal.

Employing this equality and rearranging the last equation allows the triplet concentration to be determined as follows:

$$[Chl_t] = \frac{\Delta OD_t}{b\,(\varepsilon_t - \varepsilon_g)}$$

In this equation b represents the path length through the sample and the quantity $(\varepsilon_t - \varepsilon_g)$ is referred to here as the differential extinction coefficient, which is given below. If a radical species was of interest rather than Chl_t this discussion would still hold except that parameters appropriate for the radical would have to be substituted for those used for Chl_t here.

Relative fluorescence yields were determined by estimating the area under the emission curve and normalizing to the sample with the lowest Chl concentration.

Relative mean triplet lifetimes were determined by dividing the area under the decay curve by the height of the curve at zero time. That this is an appropriate way to measure this quantity is shown by the following equations:

$$\frac{-dC}{dt} = kC$$

$$-\int_o^\infty dC = \int_o^\infty kC\,dt$$

$$-(C_\infty - C_o) = \frac{1}{\tau}\int_o^\infty C\,dt$$

$$\tau = \frac{\int_o^\infty C\,dt}{(C_o - C_\infty)}$$

where τ is the triplet lifetime (which is the reciprocal of the decay rate constant), $\int_0^\infty C\,dt$ is a measure of the area under the decay curve and $(C_o - C_\infty)$ is a measure of the signal amplitude at zero time.

For determination of absolute Chl_t yields, an extinction coefficient of 32,000 was used at 465 nm [40]. For absolute $Chl^{+\cdot}$ yields, extinction coefficients of 12,600 at 465 nm [38] and 16,650 at 395 nm were used. The latter value was calculated after having first determined the radical concentration at 465 nm. These are differential extinction coefficients, i.e., that of Chl_t or $Chl^{+\cdot}$ minus that of Chl. These are used since absorbance decreases due to depletion of Chl ground state must be considered as well as absorbances changes due to the appearance of the photoproduced species.

Chl_t quenching was analyzed according to the Stern-Volmer relationship which is shown here:

$$\frac{\tau_o}{\tau} = 1 + k_q \tau_o [Q]$$

where τ_o is the lifetime of Chl_t in the absence of quencher, τ is the lifetime in the presence of quencher, k_q is the quenching constant and [Q] is the concentration of quencher. In the case of Chl self-quenching this latter quantity was equivalent to the Chl concentration. In these experiments τ was measured at several different quencher concentrations and k_q was obtained from a plot of $\frac{\tau_o}{\tau}$ vs [Q].

The binding of BQ to liposomes was estimated by two different methods. One method involved flotation of the liposomes by centrifugation through a D_2O solution of BQ and measuring the amount of BQ

removed from the solution. Centrifugation was done at 23°C and 55,000 rpm for 140 minutes. This resulted in a banding of the liposomes at the top of the centrifuge tube. That this process did not result in any gross phase transition was indicated by the fact that gentle shaking of the tube caused resuspension of the liposome band with no appreciable increase in turbidity. In order to minimize lipid contamination, the solution, cleared of liposomes, was withdrawn by puncturing the bottom of the centrifuge tube. Absorbance due to BQ was measured at 245 nm using an extinction coefficient of 19,500 [113,114]. BQ concentrations ranged from 1×10^{-5} M to 32×10^{-5} M while the PC concentration was 1×10^{-3} M. The binding parameters were obtained using the Scatchard equation [115,116]:

$$\frac{\bar{v}}{A} = K(n - \bar{v})$$

where $\bar{v}$ is the number of moles of ligand (BQ) bound per mole of liposomes, A is the concentration of free ligand, n is the number of binding sites and K is the association constant. The concentration of liposomes was calculated assuming approximately 2,440 PC molecules per liposome [112]. Similar analysis of the binding of small molecules to liposomes has previously been done [116]. A plot of the data from a centrifugation experiment is shown in Fig. 6.

Binding was also measured by ultrafiltration [117]. Again, BQ concentrations were determined spectrophotometrically and the data subjected to Scatchard analysis. Although the data obtained with both methods showed appreciable scatter (this is due in part to the

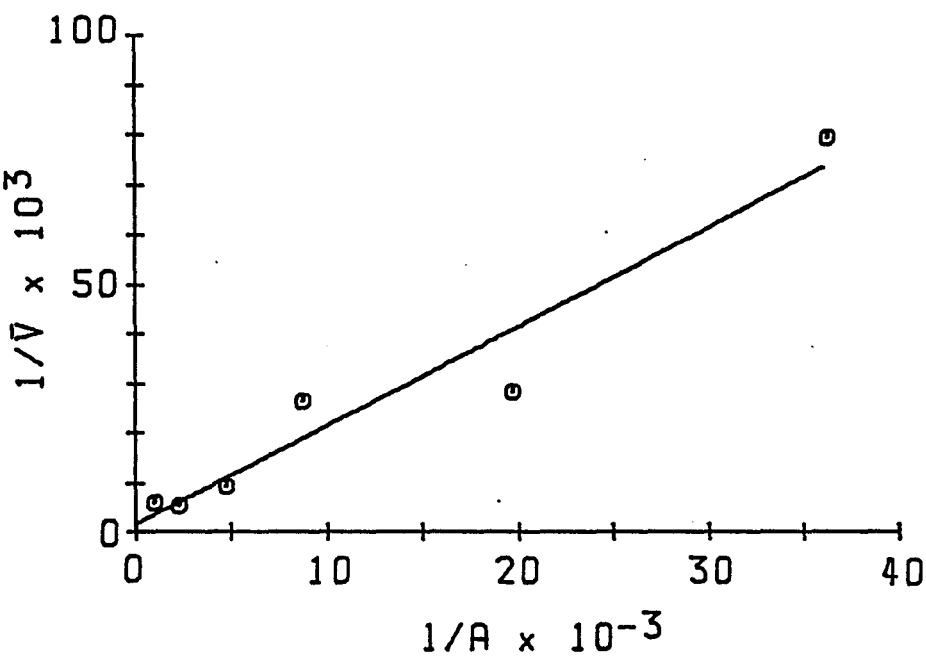

Figure 6. Scatchard plot of the binding of BQ to egg PC liposomes.

instability of BQ solutions [118]), both were in fairly good agreement with an association constant of approximately 10^3 M^{-1} and approximately 500 binding sites. These values were used in calculating BQ concentrations within the liposome phase.

CHAPTER 3

RESULTS AND DISCUSSION

The photochemical properties of the Chl-liposome system which have been investigated and described herein are divided into two main sections. First, self quenching of the Chl triplet state will be described followed by description of the electron transfer from the Chl triplet to quinone.

Self Quenching of the Chlorophyll Triplet State

The visible absorption spectrum of a Chl-liposome suspension is compared with that of a diethyl ether solution of Chl in Fig. 5. The liposome spectrum is similar to that observed in other laboratories [80,99] and demonstrates the low level of light scattering obtained with these samples. The small red shift is consistent with the Chl chromophore being in a relatively polar environment, i.e. at or near the liposome-water interface. Laser photolysis of deaerated Chl-liposomes results in a transient whose difference spectrum (Fig. 7) identifies it as the Chl triplet state (Chl_t). Consistent with this identification, the transient signal is effectively quenched by O_2. At low Chl concentrations (1 Chl/liposome), the quantum yield of triplet formation in the liposome is approximately the same as in ethanol solution, as is the fluorescence yield. (Literature values for the quantum yields of fluorescence and triplet state formation are 0.32 [in ethanol] and 0.64 [in ether] respectively [119,120].) However, under the conditions of

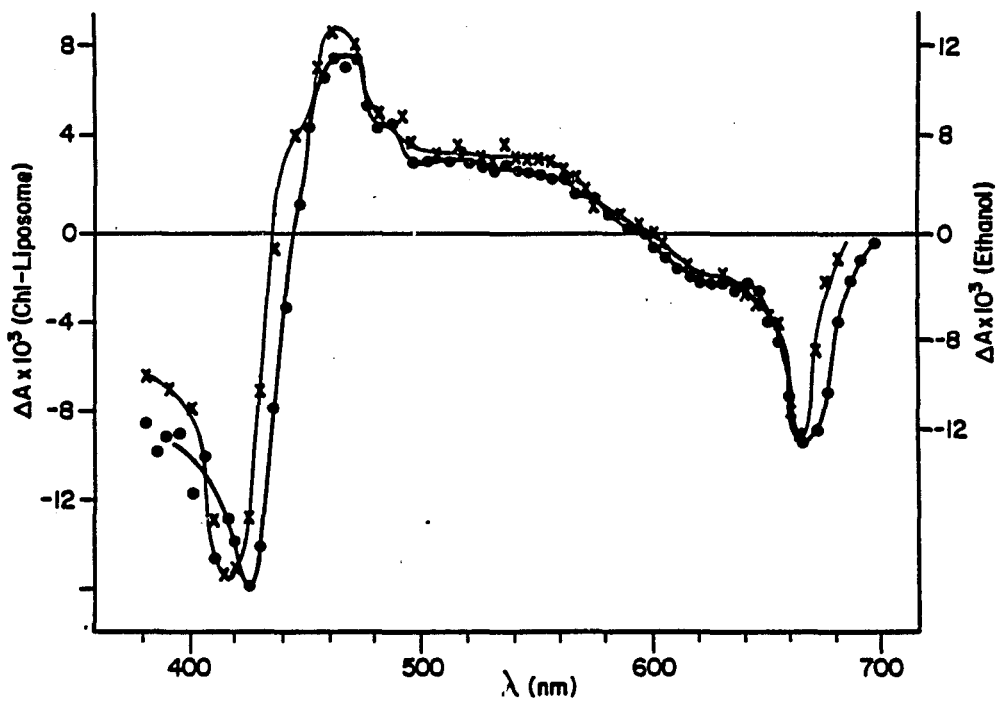

Figure 7. Difference spectrum of Chl_t.

Shown are flash-induced difference spectra in ethanol (2.5×10^{-5} M) (x—x) and in Chl-liposomes (32 Chl/liposome) (•—•). Points taken 20μs after flash.

our experiment the triplet lifetime in the liposome is significantly longer than it is in ethanol solution as shown in Fig. 8. The half-life in Chl-liposomes is 860 μs, whereas in ethanol it is 270 μs, reflecting differences in Chl-solvent interactions contributing to first-order de-excitation in the two systems. In actuality, the decay of Chl_t in solution is a mixture of first and second order processes and has been shown to obey the following equation [40]:

$$\frac{-d\ Chl_t}{dt} = k_1\ [Chl_t] + k_2\ [Chl_t]^2 + k_3\ [Chl_t]\ [Chl_g]$$

where Chl_g represents the Chl ground state, k_1 is the first order decay rate constant and k_2 and k_3 are bimolecular quenching constants due to triplet-triplet annihilation and triplet-ground state interactions respectively. Due to the possibility of these latter two quenching processes the decays plotted in Fig. 8 were taken at relatively low Chl concentrations in order to minimize Chl-Chl interactions and therefore second-order contributions. This procedure allows a more accurate determination of the first-order decay half-times from semilog plots of the decay. Triplet states of other molecules have also been shown to be stabilized by incorporation into heterogeneous systems such as liposomes and micelles. These include Zn-tetraphenyl porphyrin [121], pyrene [122], napthalene [123,124], and biphenyl [123,124]. In these cases, the stabilization was attributed to the inhibition of bimolecular radiationless decay pathways such as triplet-triplet annihilation and triplet-ground state interaction.

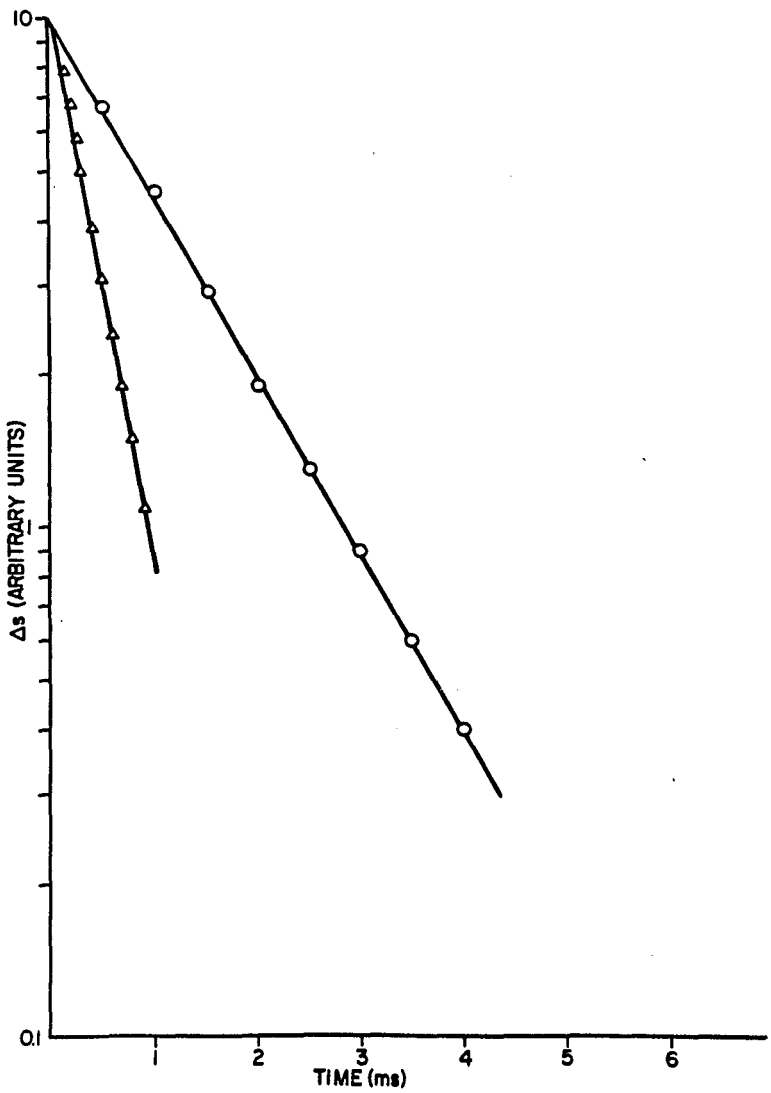

Figure 8. First order plots of the decay of Chl_t.

These represent decays in ethanol (7.2×10^{-6} M)(Δ—Δ) and in Chl-liposomes (0.26 Chl/liposome) (o—o). Monitoring wavelength is 465 nm.

In the Chl-liposome system described here, increasing the average Chl concentration in the liposome causes significant triplet quenching and deviations from exponentiality in the decay. Figs. 9 and 10 show examples of decay curves and semilog plots for Chl-liposomes at representative Chl concentrations. However, no appreciable second-order components such as triplet-triplet annihilation were detected, i.e. the shapes of the decay curves were not affected by changing the laser intensity. This is similar to a recent study [125] in which triplet states of Zn porphyrin and Zn-tetraphenyl porphyrin in vesicles comprised of dioctadecyldimethylammonium chloride were multiexponential (the overall decay appeared nonexponential however) due to triplet interactions with the ground state. In this study, similar to what was observed in our own study, the triplet decay became faster with increasing porphyrin concentration whereas at fixed porphyrin concentration the decay was independent of the laser intensity. As pointed out by these authors, the average distance between porphyrin molecules is variable (depending on the number of porphyrins solubilized per vesicle) and the quenching efficiency in each vesicle is related to this distance. This was advanced as a major reason for multiexponentiality in the decay. This concept was discussed more extensively in another paper [126] in which it was pointed out that in these types of heterogeneous systems reactive interactions take place within isolated groups of a few molecules contained in the host aggregate and for this reason rate laws which apply to reactions occurring in homogeneous solution may not strictly apply since they are based on the concept of reactive coupling between the whole ensemble of dissolved species.

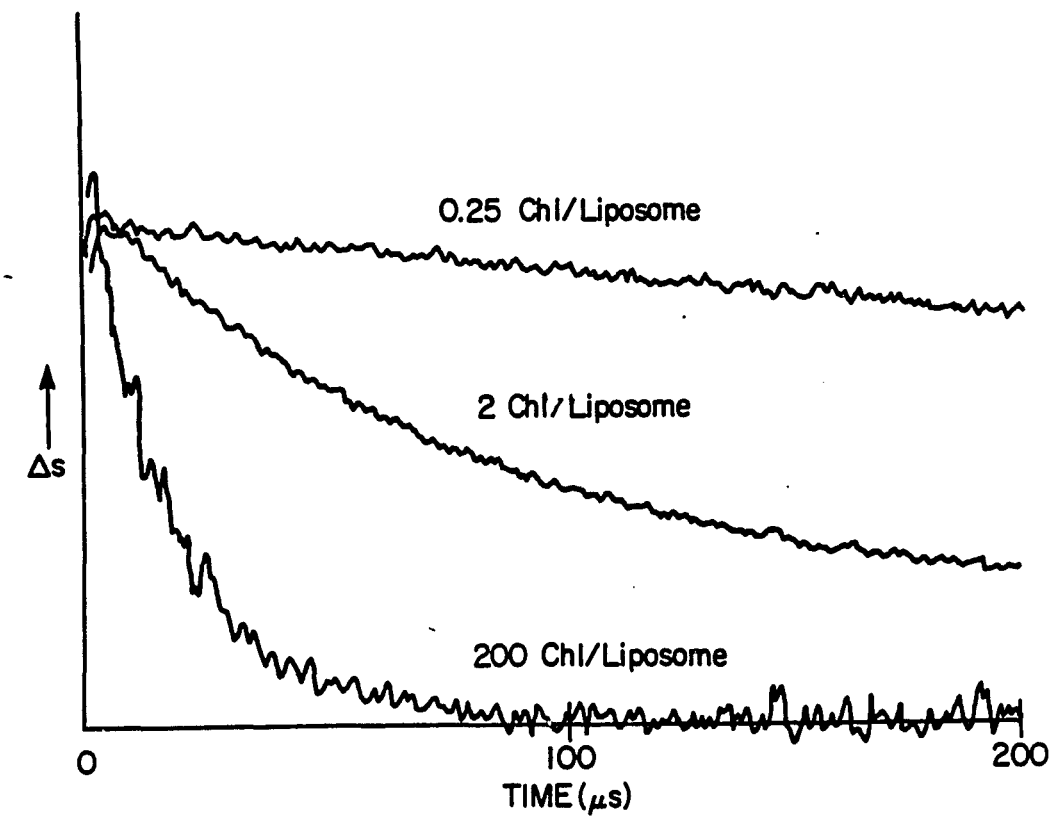

Figure 9. Decay curves of Chl_t in liposomes at various Chl concentrations.

The concentration is indicated above the decay curve. The sensitivity at 200 Chl/liposome is 4x that in the other two traces.

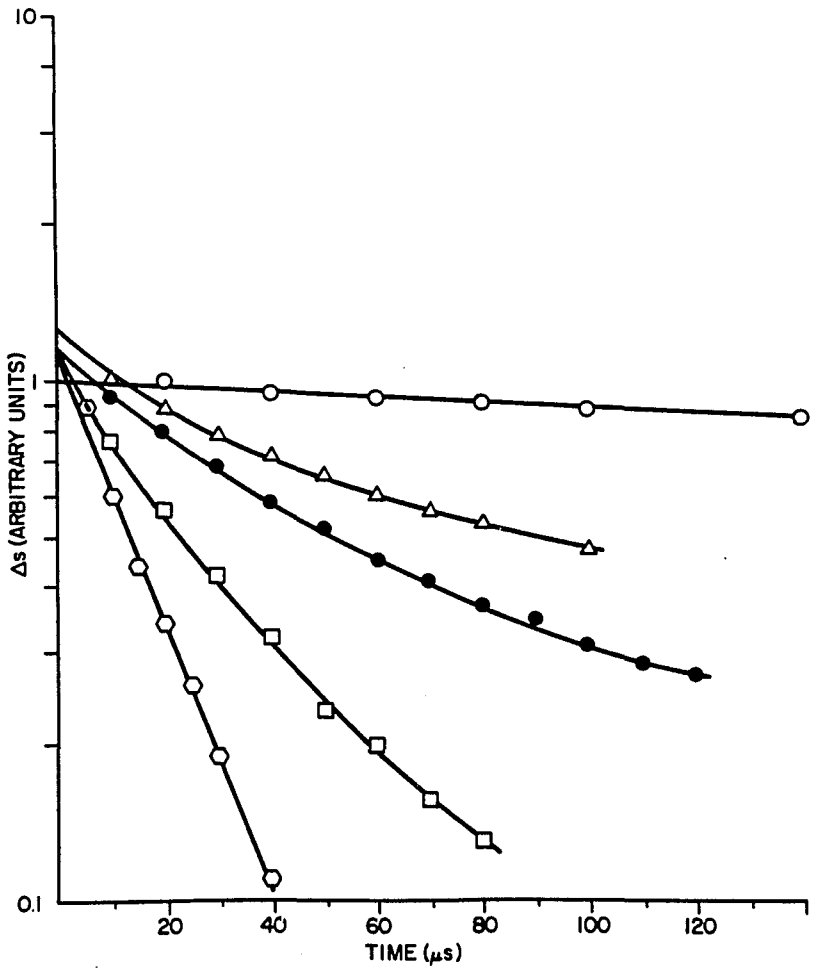

Figure 10. First order plots of the decay of Chl_t in liposomes at various Chl concentrations.

The concentrations and sensitivities are as follows:

o—o 0.26 Chl/liposome, sensitivity x1;
Δ—Δ 2.3 Chl/liposome, sensitivity x2;
●—● 5.1 Chl/liposome, sensitivity x2;
□—□ 22.8 Chl/liposome, sensitivity x4;
⬡—⬡ 200 Chl/liposome, sensitivity x8.

More specifically it was pointed out that in such systems the solubilized molecules are distributed in a statistical fashion over their host aggregates and in the excited state quenching process, host aggregates having different numbers of quenching molecules contribute differently to the events observed macroscopically. Therefore multiexponentiality would be expected. It should be noted that in our own system, deviations from exponentiality for the decay of Chl_t are observed only at intermediate concentrations, i.e. at both low and high concentrations of Chl the decays appear to be exponential. The overall nonexponential behavior at the intermediate concentrations is similarly probably due to multiexponentiality due to statistical distribution of the Chl molecules among the liposomes resulting in an overall decay which is the sum of several different decays corresponding to liposomes having varying numbers of Chl molecules. The reasons for the exponential behavior of the decays at the extremes of concentration will be discussed below.

Concentration quenching curves of the Chl singlet in liposomes has been observed and attributed to inductive resonance transfer to statistical pairs [96]. More specifically, the complexities in the decay kinetics were explained as being due to a multistep resonance transfer among identical Chl molecules, followed by transfer to the statistical pair quenching center. In Fig. 11 we report the concentration quenching curves for the triplet and singlet states as determined by laser photolysis and steady-state fluorescence respectively. Relative triplet yields are also shown. This latter quantity follows the relative fluorescence yield quite closely, as would be expected.

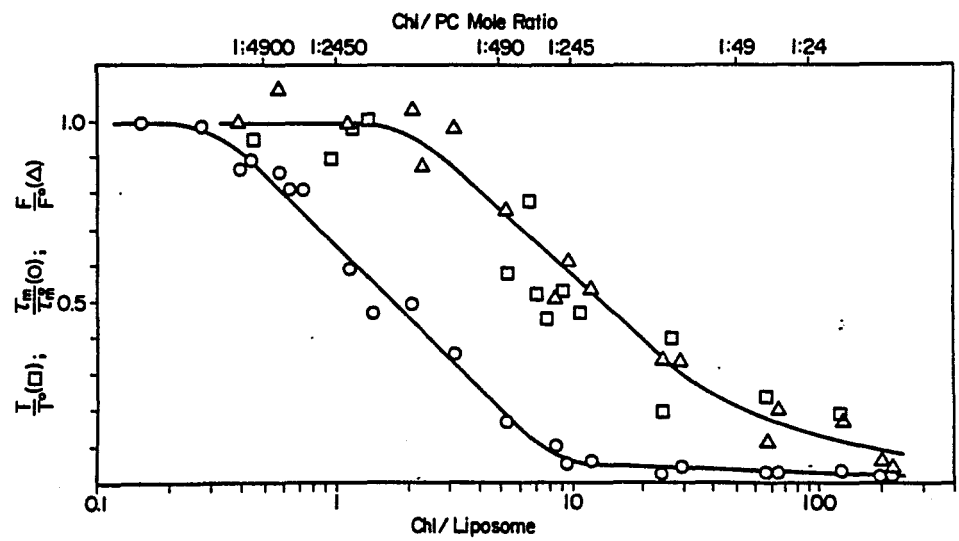

Figure 11. Concentration quenching curve of photo-excited Chl.

Shown are relative fluorescent yield, F/F_o (Δ), relative triplet yield, T/T_o ($\square$) and relative mean triplet lifetime, τ_m/τ°_m (o) as a function of average number of Chl/liposome. Calculation of these parameters is described in the text.

It should be pointed out that relative mean triplet lifetimes were calculated as described in Chapter 2. This was necessary due to the overall nonexponentiality observed in the triplet decays (a parameter such as half-time taken directly from plots of such nonexponential decays would not be an accurate measure of this quantity). The fluorescence quenching curve reported here is similar to that previously given by Beddard et al. [96]. Also in agreement with Beddard et al., we did not find any evidence of Chl aggregate formation from absorption spectral measurements in this system. It is apparent from Fig. 11 that triplet quenching becomes important at concentrations that are much lower than those necessary to quench the singlet (due to the longer lifetime of the triplet state). The above results suggest the following. Whereas the inductive resonance transfer quenching mechanism is very plausible for the singlet level, it cannot hold for triplet quenching because of the very low probability of this type of transfer from triplet state molecules. Furthermore, an exchange mechanism of triplet energy transfer can also be excluded, due to the short range nature of this process which would require the direct excitation of statistical pairs, which are present at fairly low concentrations [96]. In any case, this latter mechanism would result in quenching at the singlet level and would not affect the triplet lifetime, contrary to observation. The mechanism of quenching for the triplet must therefore be collisional, with the quenching trap being formed during the collision of triplets with ground state Chl molecules. Such a process is also observed in solution [40].

At low Chl concentrations, the decay of Chl_t would be expected to remain constant and exponential as long as the probability of having liposomes with more than one Chl, and thus quenching, is negligible. The return to exponentiality at high concentrations can be understood by realizing that at those concentrations, quenching at the singlet level becomes important and thus triplets will be formed from those singlet excited Chl molecules whose distance from a neighboring molecule is outside the interaction distance required for singlet quenching. Increasing the Chl concentration narrows the population distribution of those Chl-liposome species which are able to produce triplets, i.e. in which singlet quenching is not occurring. Beyond a certain concentration level the observed triplet decay will appear essentially exponential with a single limiting lifetime. However, the triplet yield is expected to continue to decrease. This is verified by the data in Fig. 11.

It is not unreasonable to suppose that Chl molecules are able to move within the liposome, inasmuch as lateral diffusion within bilayer membranes is a well-known phenomenon [127]. A collisional process in the Chl-liposome system is also supported by work done in this laboratory employing Chl incorporated into polymer films where diffusional processes are greatly minimized [22]. In this system, increasing the Chl concentration within the films results in a decrease in triplet yield but no change in lifetime, indicating an absence of quenching at the triplet level even though the concentration is high enough to produce singlet quenching. Furthermore, a Stern-Volmer plot (Fig. 12)

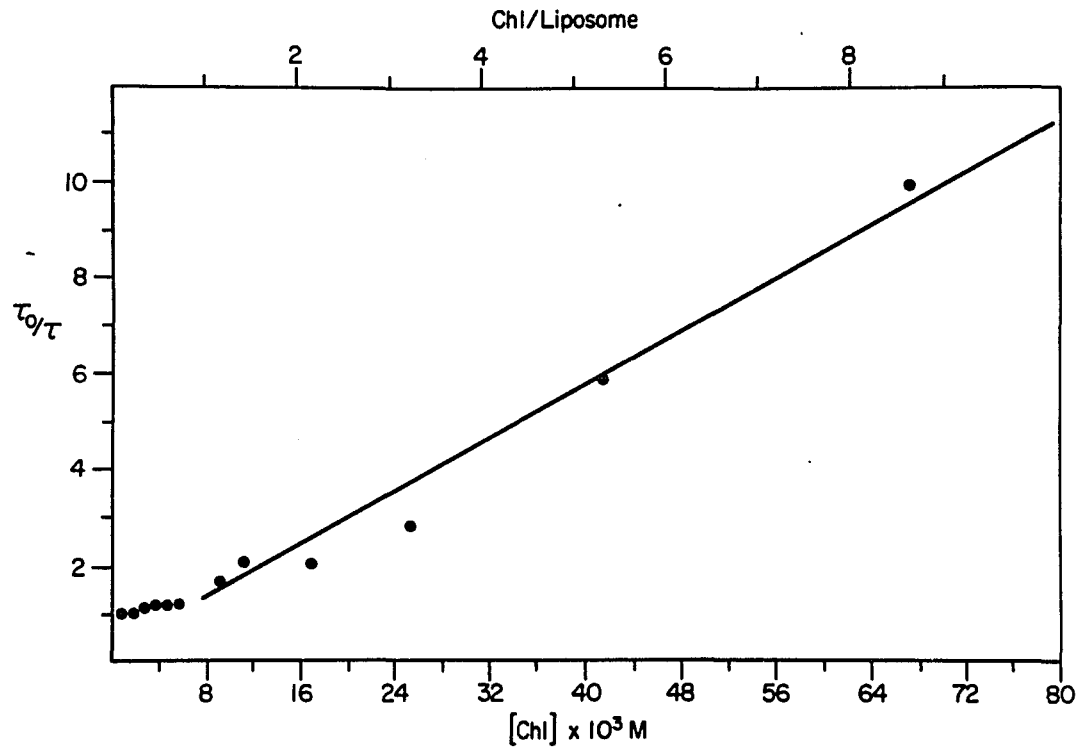

Figure 12. Stern-Volmer plot of Chl_t self-quenching in liposomes.

The Chl concentration indicated refers to that calculated for Chl within the bilayer.

of the liposome data (again mean triplet lifetimes as defined previously were employed due to the overall nonexponentiality of some Chl_t decays), which is approximately linear in the region where the major portion of the triplet quenching occurs, is likewise supportive of a diffusional quenching process (one would expect non-linearity at both ends of the concentration range). A quenching constant of 2×10^5 $M^{-1}s^{-1}$ can be calculated from these data. Assuming a diffusion coefficient of 15×10^{-9} cm^2s^{-1} for a Chl molecule, which is a reasonable value for a PC molecule in a liposome [128], a molecular radius of 15 Å, and that the viscosity of the lipid bilayer is 1 poise [129,130] the Smoluchowski equation [131] allows one to calculate a second order rate constant of 340×10^5 $M^{-1}s^{-1}$. This theoretical value is 170 times larger than the experimental value and suggests that the Chl molecules may have a more restricted mobility in the bilayer than does PC or that quenching is not diffusion controlled. It should be pointed out that the Smoluchowski equation assumes that the molecules are spherical which is certainly not the case here, the Chl molecules having their phytyl side chains in extended conformation allowing extensive intermolecular interaction with the lipid chains. Additional evidence for collisional quenching of Chl_t comes from experiments using liposomes of different fluidities where the effect of bilayer viscosity significantly affects the diffusional properties of the Chl molecules and thereby influences the quenching of Chl_t. Egg PC and DOPC exist in a fluid state at room temperature, their phase transition temperatures being below room temperature (-15° to -7° and -22°, respectively)[132]. DPPC, on the other hand, is much less fluid, its transition being above room temperature (41°C)[132]. In egg PC and DOPC, at the same

Chl:lipid mole ratios, the halftime of Chl_t is about the same (165 vs 145 μs) whereas in the less fluid DPPC liposomes, Chl_t is much more long-lived (650 μs). This increased lifetime is due to decreased collisional quenching in the more viscous bilayer.

Thus, the bilayer membrane of the liposome stabilizes Chl_t, as evidenced by a three-fold increase in the lifetime over that observed in ethanol solution. The fate of excitation energy in Chl-liposomes has been investigated and in addition to singlet state quenching which had already been substantiated [96], quenching at the level of Chl_t has now also been documented. This latter process has been shown to be due to a collisional deexcitation and therefore markedly affected by viscosity. It is therefore evident that the properties of the micro-environment in which the Chl is situated can greatly affect the fate of excitation energy in Chl assemblies and thereby affect the reactivity of Chl excited states.

Electron Transfer to Quinone

As in homogeneous solution, the quenching of Chl_t in liposomes by quinones occurs by electron transfer [133,134] and this process has also been investigated. Oettmeier et al. [101] have reported light-induced electron transfer from Chl to various quinones (as well as to other acceptors) resulting in the production of the Chl cation radical ($Chl^{+\cdot}$) and semiquinone anion radical ($Q^{-\cdot}$) which they observed using EPR spectrometry. The present studies have utilized several quinones although benzoquinone (BQ) and ubiquinone (UQ) have been most extensively investigated. Laser flash photolysis of Chl-liposomes in

the presence of quinone demonstrates that Chl_t is quenched and a more long-lived species is produced. This species has spectral properties different from Chl_t, especially in the 400 nm region, as is expected for $Chl^{+\cdot}$ [42,69]. Presumably, therefore, $Q^{-\cdot}$ is being formed as well, although it was not directly observed in these experiments. The quenching of Chl_t and the production of more long-lived species is shown in Fig. 13 for BQ. That BQ is capable of rapidly and completely penetrating the liposome is evidenced by the fact that transient decays in samples to which BQ was added following liposome formation were identical in size and shape to those in samples in which BQ was added to the buffer prior to liposome formation. In the latter case, BQ is necessarily also present in the sequestered inner aqueous compartment of the liposome and thus is able to quench those Chl molecules located in the inner segment of the lipid bilayer. This evidently occurs in the former situation as well.

The flash-induced difference spectra produced in the presence of BQ and of UQ are shown in Fig. 14. In the case of BQ two spectra are shown, one representing a rapidly decaying transient and the other a more slowly decaying species. The origin of these two decay processes is discussed below. The spectrum of the fast component is not shown in the red region due to the fact that the light scattering artifact interferes with measurements at early time points in this region of the spectrum. All three difference spectra are similar to those previously observed for $Chl^{+\cdot}$ and $Q^{-\cdot}$ in ethanol solution [135] and in cellulose acetate films [22]. The electron transfer resulting in $Chl^{+\cdot}$ production occurs from Chl_t and the concentration of $Chl^{+\cdot}$ increases steadily with

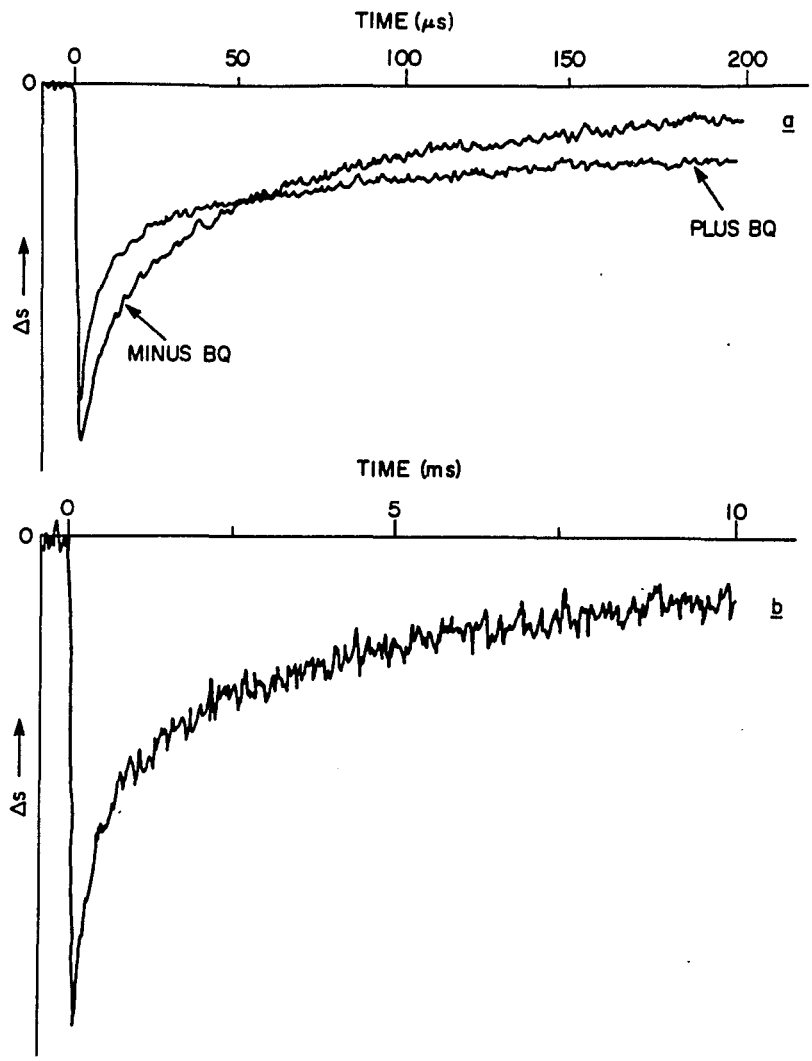

Figure 13. (a) Biphasic decay of Chl_t and Chl^+ in Chl-liposomes in the presence of BQ. (b) Decay at longer times.

The Chl concentration is 26 Chl/liposome and the BQ concentration is 5 mM. The monitoring wavelength is 665 nm. Also shown in (a) is the Chl_t decay in the absence of BQ. The sensitivity in (b) is 8x that in (a).

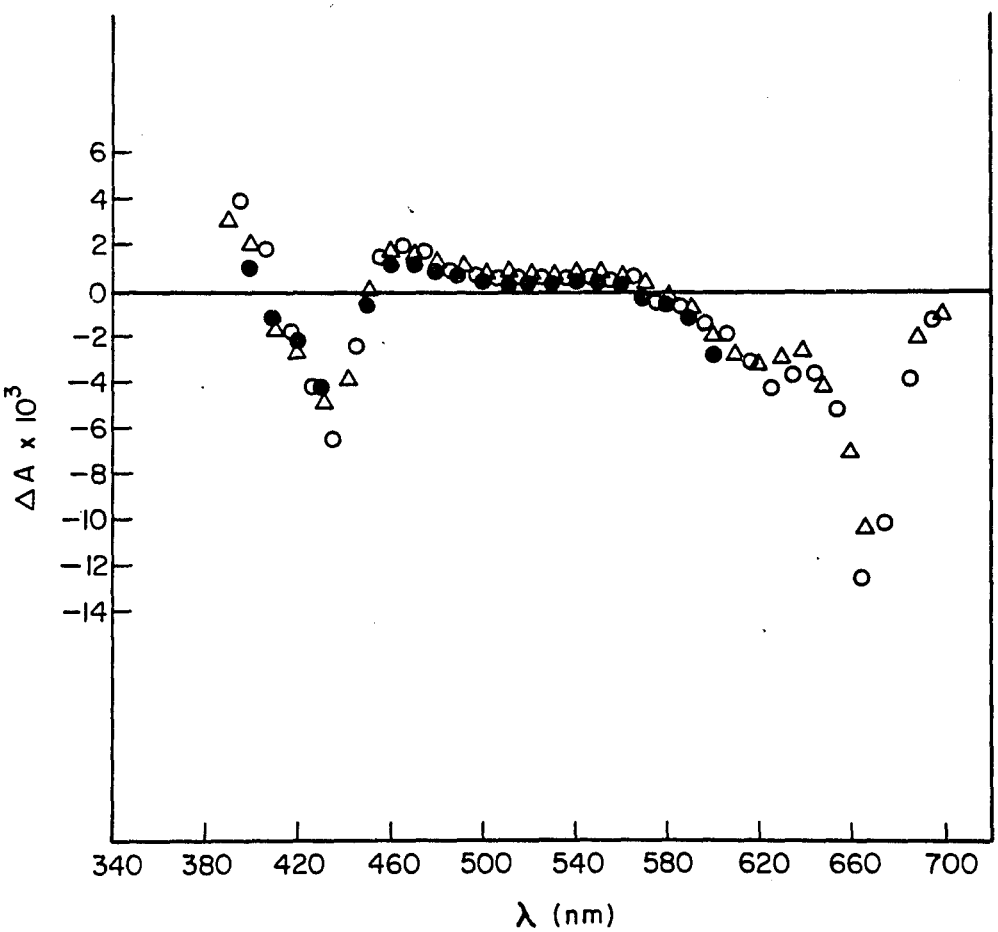

Figure 14. Difference spectrum of Chl-liposomes in the presence of quinones.

With BQ present (7.0×10^{-4} $M_{app.}$), points were taken 1 ms after the flash for the slow component (Δ) and 50 μs after the flash for the fast component (●). The absorbance at 500 μs was subtracted from this latter measurement in order to correct for absorbance due to the slow component. With UQ present (1.0×10^{-4} M_{app}) (o), points were taken at 50 μs after the flash. This sample contained 5 Chl/liposome.

increasing quinone concentration until the Chl_t concentration begins to drop due to Chl singlet state quenching. At this point the concentration of both Chl_t and $Chl^{+\cdot}$ decrease in parallel fashion as shown in Fig. 15 for an experiment in which UQ was used. Similar results were obtained with BQ. Thus, as in homogeneous solution, singlet quenching does not produce separated radicals [42,43,134]. The quenching of Chl_t by both BQ and UQ follows Stern-Volmer kinetics over the concentration range of interest (Fig. 16). The quenching constants so determined are given in Table 1. We cannot be certain as to the significance of the larger k_q for BQ in egg PC as compared to UQ, due to the uncertainty in the calculation of the BQ concentration within the vesicle. However, we feel confident that they are at least of the same order of magnitude. These values should be compared to those obtained previously (3.4×10^9 $M^{-1}s^{-1}$) for BQ in ethanol [42]. Thus, quinone diffusion is approximately 10^3 times slower within the vesicles (see below for evidence of diffusional control of triplet quenching).

The decay of the radical products obtained with BQ is biphasic (Fig. 17), indicating two decay mechanisms. Approximately 60% of the radicals decay via the slower process (the half-time for this can be as long as 40 ms). That the faster decaying species is in fact $Chl^{+\cdot}$ and not unquenched Chl_t is shown by the following: its spectrum is the same as the slower species, the halftime of the decay is independent of the Chl concentration and the decay time is not shortened by the presence of oxygen. The concentration of both species is, however, significantly decreased in the presence of O_2, consistent with the precursor role of Chl_t in electron transfer.

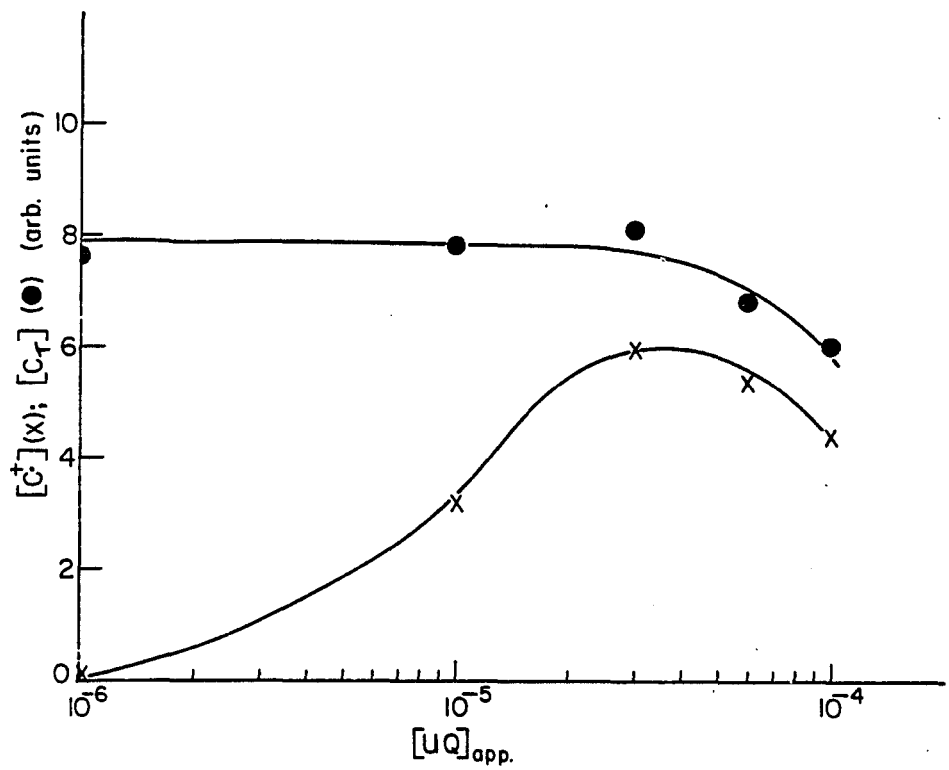

Figure 15. $Chl^{+}_{\cdot}$ and Chl_t yields as a function of UQ concentration.

$Chl^{+}_{\cdot}$ yields were obtained by extrapolating semilog plots of the decay curve at 395 nm back to zero time whereas Chl_t yields were obtained in similar fashion at 465 nm. This sample contained 5 Chl/liposome.

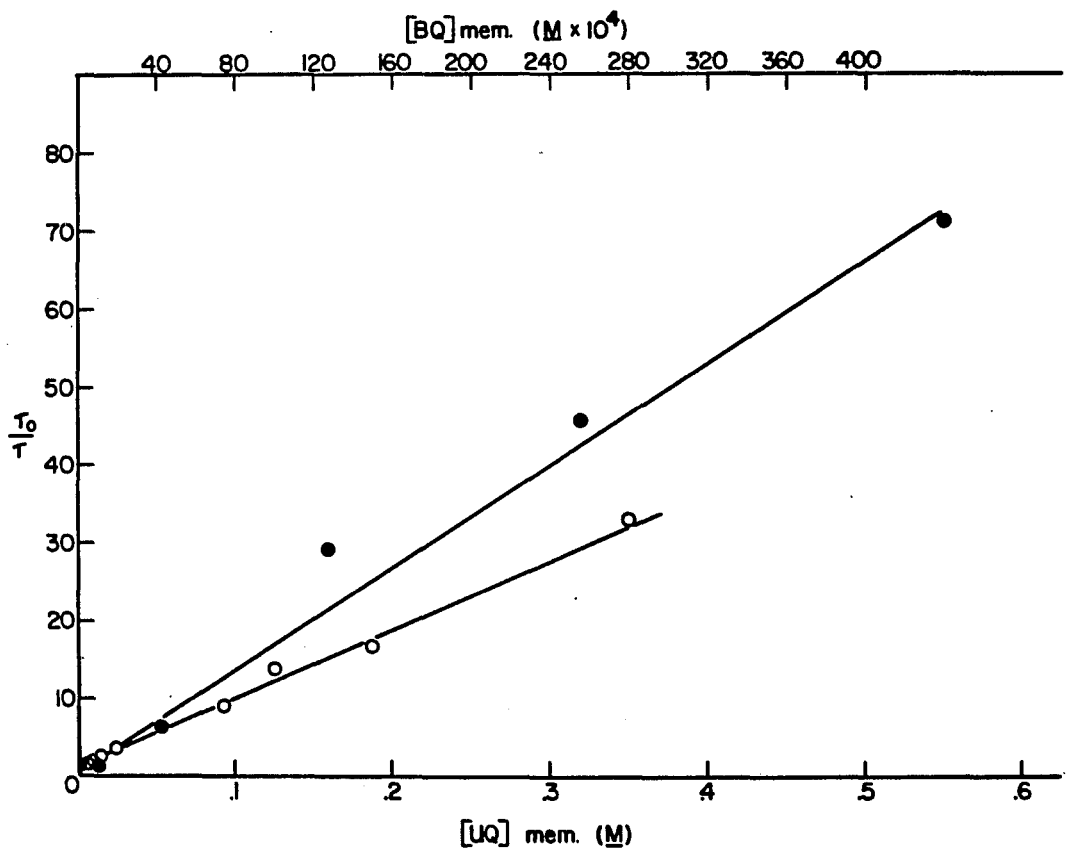

Figure 16. Stern-Volmer plots of Chl_t quenching by BQ (•) and UQ (o). The values of τ_o were 160 μs and 55 μs respectively.

Table 1. Electron transfer to quinones in various lipid bilayers.[a]

Quinone	Redox Potential(V)	Lipid	$k_q x10^{-6}$ ($M^{-1}s^{-1}$)	Maximal %Conversion $Chl_t \rightarrow Chl^+$	%Fast	%Slow
BQ	-0.510[b]	egg PC	7.2	60	40	60
		DOPC	nd[d]	70	50	50
		DPPC	nd	70	40	60
UQ	-0.840[c]	egg PC	2.2	15	100	0
		DOPC	1.7	13	100	0
		DPPC	0.3	0	0	0
DQ	-0.840[b]	egg PC	1.2	60	50	50
DTBQ	-0.730[b]	egg PC	2.0	30	50	50

[a] The Chl:PC mole ratio was 1:500 in all cases.

[b] Data taken from ref. 136.

[c] Data taken from ref. 137.

[d] nd signifies a quantity not determined.

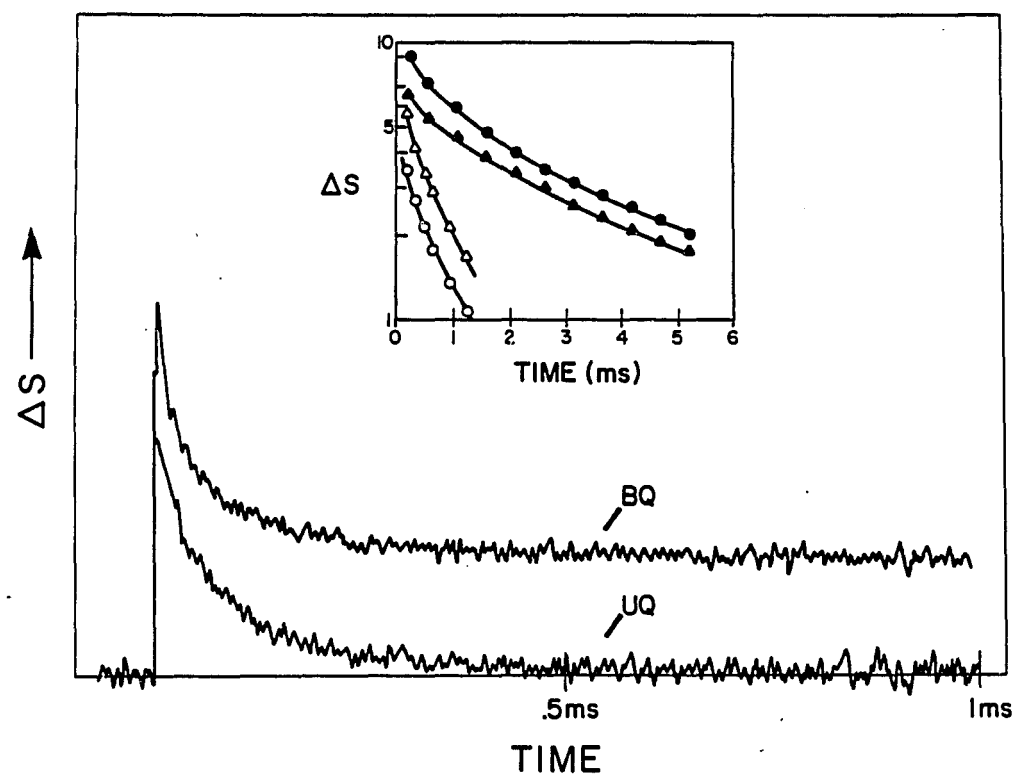

Figure 17. $Chl^{+\cdot}$ decays with quinone present.

These decays were taken at 395 nm with either BQ (5 $mM_{app.}$) or UQ (1 x 10^{-5} $M_{app.}$). The inset shows a semilog plot of these data for BQ (●) and UQ (Δ) as well as the data obtained after cutting the laser intensity by a factor of 4 and 3 for BQ (▲) and UQ (o) respectively. This sample contained 5 Chl/liposome.

The overall percent conversion of Chl_t to $Chl^{+\cdot}$ which is obtainable is 60 ± 10%, including both the fast and slow components. The $Chl^{+\cdot}$ yield closely follows that of the triplet (Fig. 18) indicating that at the quinone concentration used the Chl concentration does not affect the efficiency of conversion of Chl_t to $Chl^{+\cdot}$. The conversion obtained in Chl-liposomes is slightly less than the 70 ± 10% conversion observed in ethanol solution [42] and larger than the 25-30% obtained in cellulose acetate films [22]. However, the half-time for the decay of $Chl^{+\cdot}$ can be approximately 1900 times slower in Chl-liposomes (for the slow decay process) than it is in ethanol solution. This value is obtained from the fact that a sample having 0.74 Chl/liposome and an initial $Chl^{+\cdot}$ concentration of 5.4×10^{-4} M (within the membrane) decays with a half-time of 1.7 ms. In an ethanol solution, this concentration of $Chl^{+\cdot}$ would be expected to decay with a half-time of 0.9×10^{-3} ms. Thus, in the liposome as is also the case in the cellulose acetate films [22], radical lifetimes are increased much more than triplet conversion is diminished. This is of significance with respect to the efficiency with which photochemical energy conversion in these systems can potentially be utilized to perform useful work.

When UQ is employed as acceptor only one decay process is observed (Fig. 17). It is evident that the rate of this decay ($t_{1/2}$ approx. 150 μs) is similar to that of the rapidly decaying radical observed with BQ as acceptor. The biphasic decay observed with BQ is most probably due to the fact that this compound can partition into the membrane [138] (i.e., it has a finite solubility in both hydrophilic and lipophilic solvents). On the other hand, UQ, a highly lipophilic

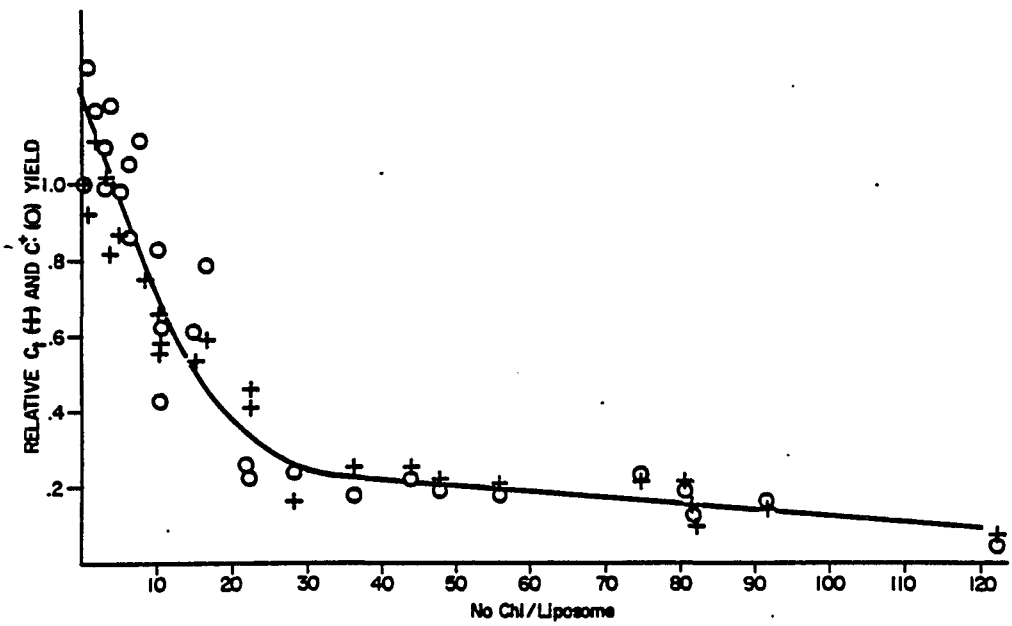

Figure 18. Relative Chl_t and Chl^+ yields as a function of average number of Chl/liposome.

The data were obtained by extrapolating decay curves to zero time. All yields were normalized to the value for the sample having the lowest Chl concentration (0.74 Chl/liposome). The absolute concentrations for this sample were 1.7 μM (Chl_t) and 1.2 μM (Chl^+).

quinone, is constrained to be situated within the bilayer. We thus attribute the faster decay process observed with both quinones to recombination of $Chl^{+\cdot}$ and $Q^{-\cdot}$ occurring within the membrane. The more slowly decaying $Chl^{+\cdot}$ is due to recombination across the interface, i.e. with external $BQ^{-\cdot}$ located at the H_2O-bilayer interface.

The radical decay rate constants observed using either BQ or UQ as electron acceptor do not change (Fig. 17 inset) upon decreasing the laser intensity (and therefore the initial concentration of reactive radicals). This feature is characteristic of first-order reaction kinetics which describe intramolecular processes and also geminate recombination reactions [139,140]. Geminate recombinations are those in which the two species never become independent of one another and therefore react as a pair. If these species did become independent of each other they could then randomly diffuse throughout the entire ensemble of reactive species and second order kinetics should obtain. In our case the invariance of decay rate constant for the reverse electron transfer reaction with respect to changes in laser intensity is primarily due to the fact that the vast majority of liposomes experience no more than one electron transfer reaction and radical products in a particular liposome back react with a rate constant characteristic of that liposome. The rate of this intra-liposomal process changes from one liposome to the next depending on such variable factors as liposome size (i.e. reaction volume) and diffusional characteristics (which can be affected by the concentration of other molecules solubilized by the liposome). Thus, it might be expected that if we had a completely homogeneous population of liposomes

in terms of both liposome size and distribution of Chl and quinone molecules among the liposomes, first order kinetics would be observed (even though this reaction is bimolecular) as long as the number of liposomes having more than one pair of radicals was negligible (otherwise second order kinetics would be observed). In this case exponentiality in the decay would be observed and an analogy to geminate recombination or intramolecular processes would be perfectly valid. The distribution of molecules among liposomes and the size distribution of liposomes would cause the overall radical decay to be multiexponential. This is somewhat analagous to the decay of Chl_t discussed previously. Also, multiple electron exchanges and a distribution of separation distances between $Chl^{+\cdot}$ and $Q^{-\cdot}$ would likewise contribute to non-exponentiality. These latter two possibilities do exist in view of the mechanism of radical formation and decay which includes interquinone electron exchange as discussed below.

Concerning the biphasic nature of the $Chl^{+\cdot}$ decay, it should be pointed out that a similar biphasic decay has been observed in a system where an amphiphathic ruthenium complex solubilized in a PC liposome photo-oxidized N,N-dimethylaniline (DMA) [141]. These authors reported that both decays followed second-order kinetics, although apparently no experiments were done at varied flash intensities. The fast decay was attributed to direct recombination of radicals while no extensive attempt was made to explain the slower decay except that the possibility of distal interliposome migration of DMA^+ was mentioned. The fact that we do not observe any second-order behavior in the radical decays allows us to rule out such an interliposomal process.

The decay rate of the slow component of the $Chl^{+\cdot}$ decay in liposomes is independent of Chl concentration but increases with increasing quinone concentration (Fig. 19). The fast decay, as evidenced by the $Chl^{+\cdot}$-$UQ^{-\cdot}$ recombination, is independent of both of these parameters (Fig. 20). The surprising result here is the dependence of the slow decay on quinone concentration. This can be understood if one assumes the mechanism shown in Fig. 21 for the production and decay of this species. We suggest that $Q^{-\cdot}$ to Q electron transfer can occur in both the forward (radical formation) and reverse (radical recombination) reactions (more direct evidence for this is given below). Increasing the BQ concentration will then serve to increase the number of quinone molecules which can function as intermediates in the reverse electron transfer reaction. This allows a greater number of possible return routes by which the external $BQ^{-\cdot}$ can transfer its electron back to $Chl^{+\cdot}$ in the membrane and results in an increase in rate for the slowly decaying $Chl^{+\cdot}$ upon increasing the BQ concentration. The concentration independence of the rate of the fast decay component implies that the rate-limiting step is the $Q^{-\cdot}$ to $Chl^{+\cdot}$ electron transfer, as opposed to any secondary electron transfer steps involving Chl or Q. Similarly, the fact that the slow decay is independent of Chl concentration indicates that any Chl to $Chl^{+\cdot}$ electron transfer that may be occurring is not rate-limiting. As an extension of these arguments, we can conclude that the rate limitation for the slow decay process must be the transfer which occurs across the bilayer-water interface.

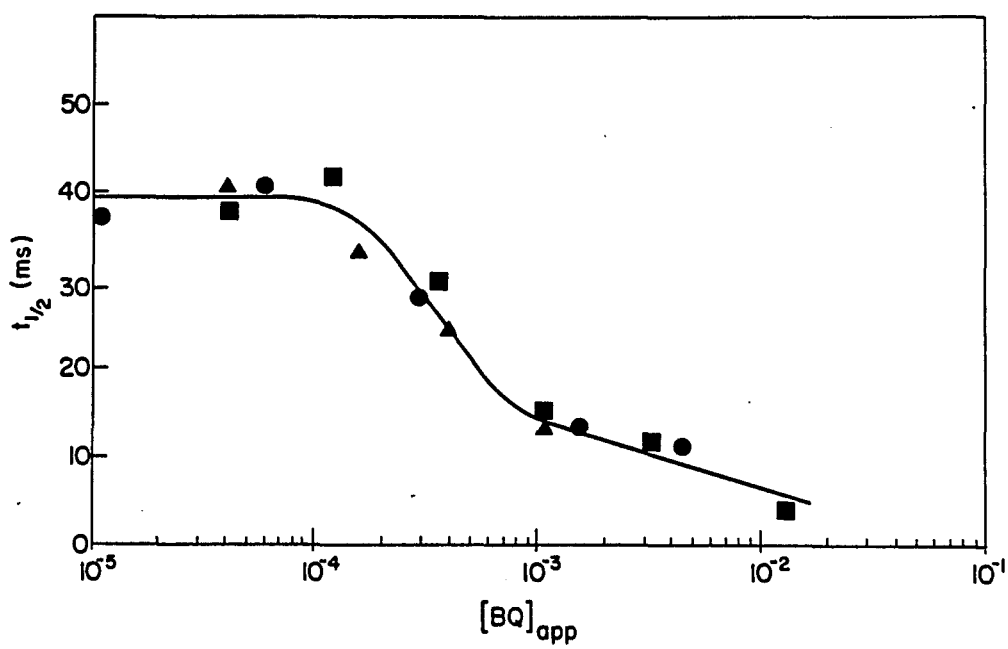

Figure 19. Dependence of the slow component of the Chl^{+} decay on the apparent BQ concentration.

These data are from semilog plots of 395 nm traces with the slow decay being extrapolated to zero time. Shown are data for samples containing 1 (●), 5 (■) and 30 (▲) Chl/liposome.

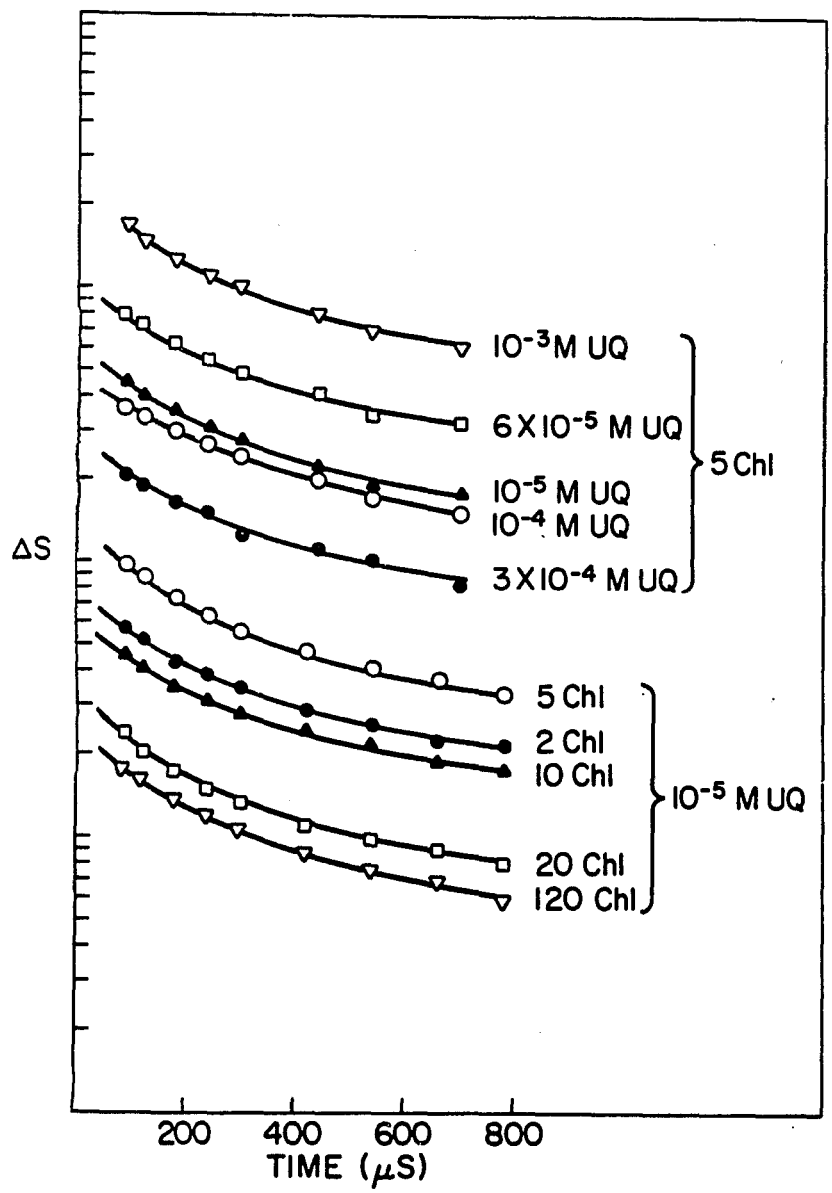

Figure 20. Invariance of the decay rate of fast component of the Chl^{+} decay as a function of Chl and UQ concentrations.

These data are from 395 nm traces. Chl concentrations (in terms of number of Chl/liposome) and apparent UQ concentrations are shown. The intensities of these plots are not comparable.

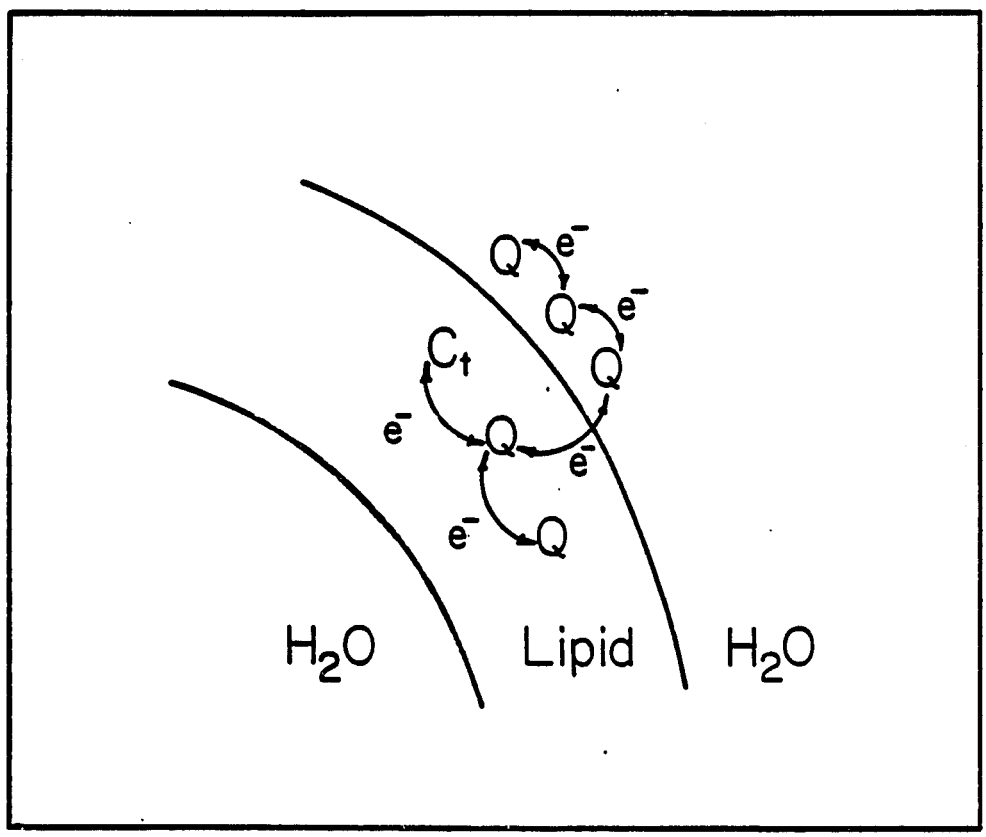

Figure 21. Hypothetical scheme for electron transfer between Chl and quinones in liposomes.

Figure 22 shows the $Chl^{+\cdot}$ yield as a function of apparent concentration of UQ, DQ and BQ. The relative positions of these curves is consistent with the partitioning of each quinone between the aqueous and liposome phases. Thus, UQ, which is water insoluble, achieves its maximum $Chl^{+\cdot}$ yield at a much lower apparent concentration than does BQ which has an appreciable water solubility. DQ, only slightly water soluble, is intermediate but closer to UQ in this effect. More revealing in terms of mechanistic arguments is that the midpoint of the yield in the case of BQ occurs at a much lower concentration than does the midpoint of the $Chl^{+\cdot}$ halftime dependence (0.2×10^{-4} vs 6×10^{-4} M, Fig. 19). That the yield reaches half its maximum value at lower concentrations indicates that additional quinone in this region is still penetrating the membrane and contributing to the internal membrane electron transfer reaction. As this saturates, further addition of quinone will act to increase the interfacial quinone concentration, thereby increasing the effect on the slow return pathway, which shows up as an increase in the slow $Chl^{+\cdot}$ decay rate.

Studies of these electron transfer processes in bilayers of different fluidities clearly show the effects of viscosity. Table 1 presents triplet quenching constants and conversion efficiencies for radical production in bilayers of different composition. As stated previously, egg PC and DOPC exist in a fluid state at room temperature, whereas DPPC is much less fluid. These fluidities (viscosities) are reflected in Chl_t decay half-times at the same Chl-lipid mole ratios. In egg PC and DOPC, the half-time is about the same (165 vs. 145 μs) while in DPPC, Chl_t is much more long-lived ($t_{1/2}$ = 650 μs). The

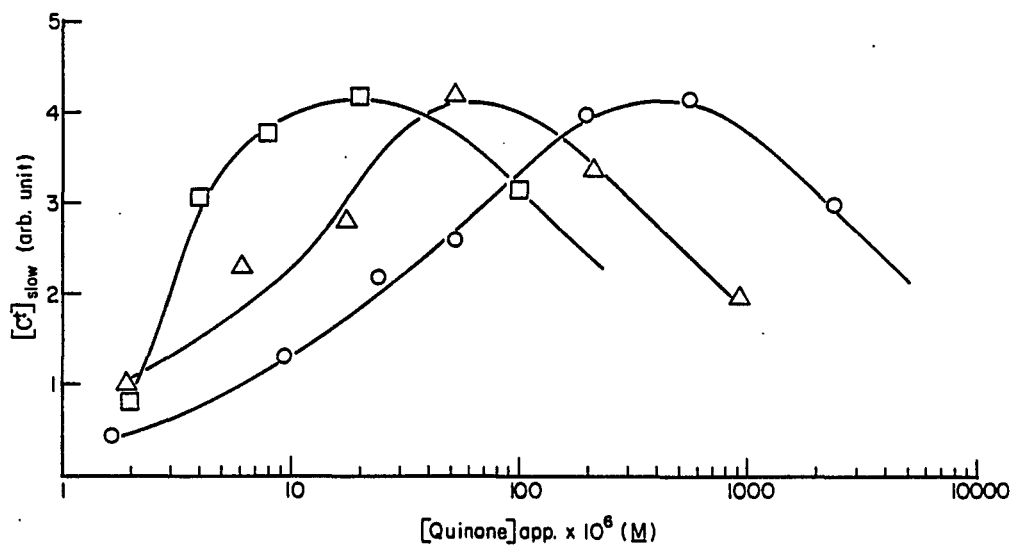

Figure 22. Concentration of $Chl^{+\cdot}$ produced as a function of quinone concentration.

Data obtained with UQ (□), DQ (Δ) and BQ (o) are shown. In the cases of DQ and BQ it is the slow component that is shown. The data were obtained by extrapolating semilog plots of 395 nm traces to zero time. Each sample contained 5 Chl/liposome.

increased lifetime is due to decreased collisional quenching in the more viscous bilayer. A viscosity effect also appears in the quenching of Chl_t by UQ (as would be expected for a diffusional process) as well as in the radical conversion efficiencies. Thus, the quenching constants (Table 1) are similar in egg PC and DOPC but substantially smaller in DPPC. The triplet to radical conversion efficiencies reflect this same effect: 15% conversion in egg PC and 13% in DOPC, while no measurable radical at all is produced in DPPC. The fact that no $Chl^{+\cdot}$ is produced from UQ in DPPC is presumably due to an internal viscosity high enough to prevent $UQ^{-\cdot}$ from diffusing away from the radical-pair complex before reverse electron transfer occurs. The conversion efficiencies obtained when BQ was employed as acceptor are similar in all three lipids (approximately 60-70%). That we observe no appreciable reduction in radical yield in DPPC with BQ implies that this quinone, being a much smaller molecule than UQ (108 vs. 591 MW), and having no long hydrocarbon tail, is still able to diffuse away from the electron transfer site with high efficiency. There is however, an appreciable decrease (approximately two times) in the fast $Chl^{+\cdot}$ decay rate in DPPC (Fig. 23). Thus, radical pair separation with UQ is much more dependent on viscosity than is recombination with BQ.

Figure 24 shows the concentration of radical produced as a function of the fraction of Chl_t quenched $(1 - \tau/\tau_o)$. For a simple one-step mechanism, i.e., electron transfer followed by radical-pair separation, a linear relationship would be expected. The non-linear dependence which we obtain (this was also found with DQ) implies a cooperativity among quinone molecules in producing $Chl^{+\cdot}$. The

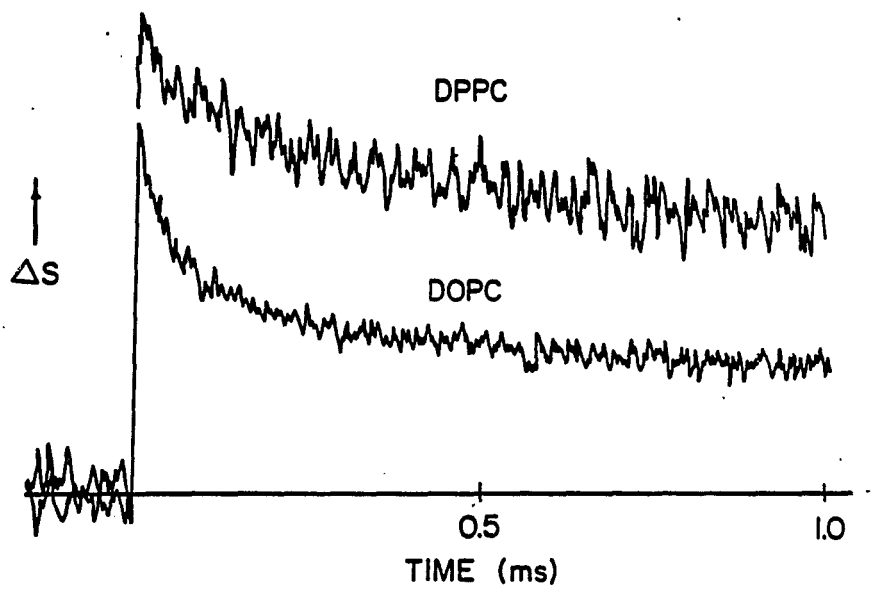

Figure 23. Decay of $Chl^{+\cdot}$ in DPPC and DOPC liposomes.

These traces were obtained using apparent BQ concentrations of 1.1 and 0.8 mM respectively. The monitoring wavelength is 395 nm. Both samples contained 5 Chl/liposome.

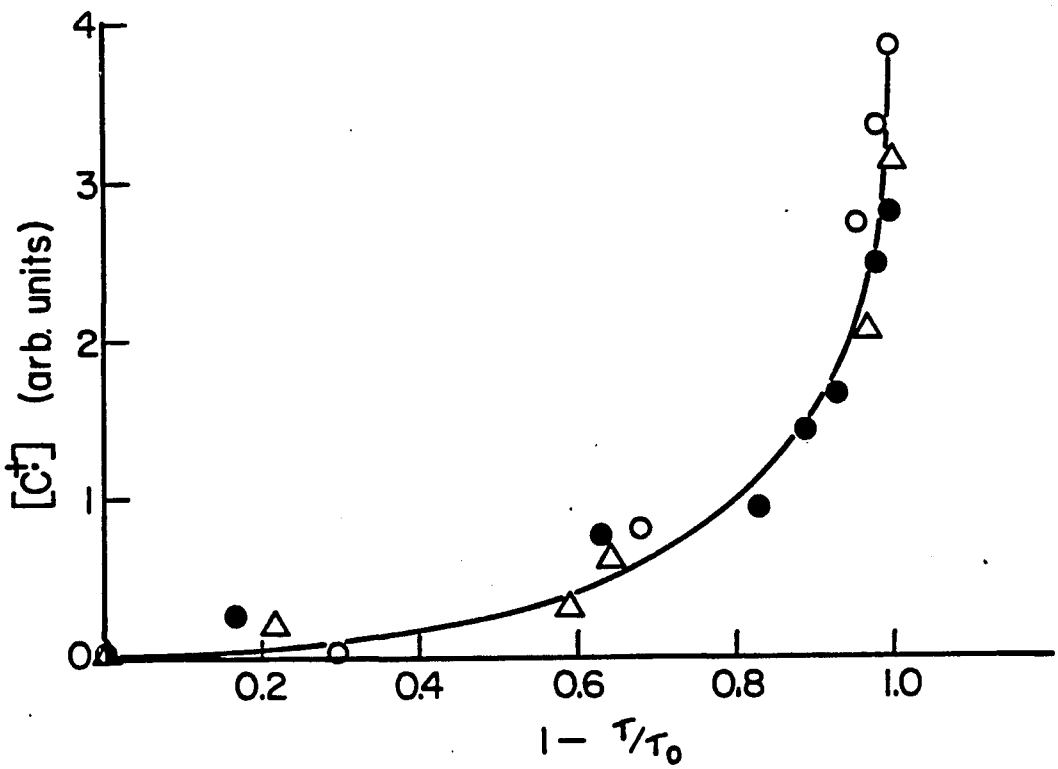

Figure 24. Concentration of $Chl^{+\cdot}$ produced as a function of the fraction of Chl_t quenched $(1 - \tau/\tau_o)$.

Data for BQ (•), UQ (o) and DTBQ (Δ) are shown. In the cases of BQ and DTBQ it is the concentration of the slow component that is shown. The data are from semilog plots extrapolated to zero time.

mechanism presented in Fig. 21 includes $Q^{\cdot -}$ to Q electron transfer in the forward reaction and we believe that this is responsible for the cooperativity that we observe. In other words, efficient radical pair separation requires $Q^{\cdot -}$ to Q electron transfer in order to effectively compete with recombination. A somewhat similar mechanism has been described previously [142,143] in micellar systems where a photochemically reduced transition metal ion at the micelle surface exchanges with an unreduced ion present in relatively high concentration in the Gouy-Chapman layer. This exchange mechanism is ultimately equivalent to the electron transfer mechanism we propose, with both leading to a cooperative and efficient means of charge separation. Such an electron transfer mechanism as we propose has been well characterized for many organic free radical systems including several quinone systems [144-147]. It might also be pointed out that Hauska [148] has postulated domain formation of UQ in PC liposomes, an effect which might readily lead to the cooperativity which we observe.

Still further evidence for interquinone electron transfer is given by the results in Table 2. In this experiment, BQ was added to an egg PC liposome sample which contained enough UQ to highly quench (98%) Chl_t. Even at 10^{-6} M added BQ, an appreciable amount of slowly decaying radical was produced. At the lowest (micromolar) BQ concentrations, the results suggest that the slow $Chl^{+\cdot}$ was formed at the expense of the fast $Chl^{+\cdot}$, i.e., upon going from 1×10^{-6} to 9×10^{-6} M BQ, the total $Chl^{+\cdot}$ remained essentially constant but the proportion of fast to slow $Chl^{+\cdot}$ decreased. It should be pointed out that in the experiment with no UQ present, we were not able to accurately estimate

Table 2. Radical production and triplet quenching parameters indicating quinone-quinone electron transfer.[a]

$[UQ]x10^5M$	$[BQ]x10^6M$	$1-\tau/\tau_o$	τ_o/τ	$[Chl^+\cdot]$ (arbitrary units)		
				Total	Fast	Slow
0	0	0	1.0	0	0	0
0	1	0.01	1.0	nd[b]	nd	8
0	3	0.28	1.3	nd	nd	14
0	9	0.65	2.8	nd	nd	25
0	50	0.90	10.4	64	20	44
0	100	0.96	25.4	96	47	49
2	0	0.98	50.8	18	18	0
2	1	0.98	52.7	23	20	3
2	3	0.98	52.1	22	16	6
2	9	0.98	52.3	22	14	8
2	50	0.98	64.4	46	25	21
2	100	0.98	82.6	60	28	32

[a] The Chl:PC mole ratio was 1:500 in all cases.

[b] nd signifies not determined.

the concentrations of total and fast $Chl^{+\cdot}$ at the lowest BQ concentrations because of the overlap of the Chl_t (which is still present in significant concentration) and $Chl^{+\cdot}$ spectra. When one considers that the Chl_t decay rate at these concentrations of UQ is approximately fifty times faster than it is with no UQ present, the amount of slow $Chl^{+\cdot}$ produced is far greater than one would expect if BQ were reacting directly with Chl_t (for example, in the absence of UQ, 10^{-6} M BQ has virtually no effect on the Chl_t lifetime; thus, it could not compete with UQ as a triplet quencher). The above results provide strong support for the inclusion of $Q^{-\cdot}$ to Q electron transfer in the mechanism of radical formation depicted in Fig. 21. It is interesting that a similar type of electron transfer is operative in photosynthetic systems [149].

Several other quinones have also been looked at in terms of quenching and conversion efficiencies and proportion of fast and slow radical components and these results are shown in Table 1. For duroquinone (DQ), which has a redox potential equal to that of UQ but no long hydrocarbon tail, we observe a much higher conversion efficiency than is seen with UQ as well as the production of substantial slow radical. This further demonstrates the effect of diffusion on radical pair separation. DTBQ, which also has a relatively low redox potential, shows a reduced conversion efficiency, although not as low as with UQ. Since this smaller molecule would be expected to diffuse more readily than UQ, we attribute the lower yield to steric hindrance or to some combination of steric and diffusional properties which inhibit a productive encounter complex leading to subsequent electron transfer.

Again, however, a substantial slow radical signal was observed. The fact that slowly-decaying radical and the quinone concentration dependence of the decay rate was observed with all of the quinones used, with the exception of UQ, suggests that the important factor in allowing this pathway of radical decay is the mobility of the quinone within the vesicle, rather than the degree of water solubility. Presumably, the anchoring of UQ by its hydrocarbon tail prevents it from assuming the required orientation within the interface region.

Concluding Remarks

Lipid bilayer vesicles (liposomes) containing Chl molecules are being extensively studied in a number of laboratories since they represent an important model system for investigating various aspects of the *in vivo* photosynthetic process. Work in these and similar types of models is a natural extension of research both past and ongoing in homogeneous solution. At present considerable information is available concerning the structure and excited state dynamics of these systems. This, as well as potential practical applications stemming from the possibility of employing Chl in a photochemical energy conversion device, has been discussed extensively in the introduction section of this dissertation. The results which have been presented deal with the fate of excitation energy and electron transfer to quinones within Chl-liposomes. More specifically, the self quenching of the Chl excited state and the mechanism of formation and decay of the radical species generated by light-induced electron transfer from the Chl triplet to various quinones has been documented.

As evidenced by a three-fold increase in the lifetime over that observed in ethanol solution, the bilayer membrane of the liposome stabilizes the Chl triplet state. The relative triplet yield follows the relative fluorescence yield, indicative of quenching at the singlet level. Triplet state lifetimes are markedly shortened as the Chl concentration is increased, demonstrating that quenching occurs at the triplet level as well. This process was shown to be due to a collisional de-excitation as is true of the analagous process occurring in homogeneous solution [40].

Chl triplet quenching by quinone was controlled by diffusion occurring within the bilayer membrane (k_q $\sim 10^6$ $M^{-1}s^{-1}$ as compared to $\sim 10^9$ $M^{-1}s^{-1}$ in ethanol), with the reduced rate constants reflecting bilayer viscosity. This quenching process results in electron transfer and the formation of relatively long-lived radical products. Radical formation via separation of the intermediate ion pair is also inhibited by increased bilayer viscosity. Cooperativity was observed in the radical formation process due to an enhancement of radical separation by electron transfer from semiquinone anion radical to a neighboring quinone molecule. This is significant in that a similar process is known to occur in vivo whereby $UQ^{\cdot -}$-UQ electron exchange is involved in transferring the electron from the initially reduced UQ to the UQ pool in photosynthetic bacteria [149].

Two modes of radical decay have been observed, a rapid ($t_{1/2}$ = 150 μs) recombination between chlorophyll and quinone radicals occurring within the bilayer and a much slower ($t_{1/2}$ = 1-100 ms) recombination occurring across the bilayer-water interface. The latter

was also cooperative, which accounts for a $t_{1/2}$ which is dependent upon quinone concentration. The slow decay was only observed with quinones which were not tightly anchored into the bilayer, and is apparently the result of electron transfer from semiquinone anion radical formed within the bilayer to a quinone molecule residing at the bilayer-water interface. Direct evidence for such a process has been obtained from experiments in which both ubiquinone and benzoquinone are present simultaneously. With benzoquinone, approximately 60% of the radical decay occurs via the slow mode. Triplet to radical conversion efficiencies in the bilayer systems are comparable to those obtained in fluid solution (∿60%). However, radical recombination, at least for the slow decay mechanism, is considerably retarded.

Due to its membranous nature it is apparent that the model system employed in the studies described here is relevant to the functioning of Chl in its biological environment. Although it would appear unlikely that a simple model like Chl incorporated into liposomes would duplicate exactly the detailed environment and physical state of Chl <u>in vivo</u>, certain aspects of the photosynthetic process (such as Chl photooxidation and acceptor reduction) have been observed in model systems and further studies with regard to these processes and others pertaining to photosynthesis can be carried out. For instance, since it is known from solution studies that solvent dielectric properties can profoundly affect this electron transfer reaction, it would be of interest to ascertain the effect of bilayer surface charge on the reaction in liposomes. Thus one might expect an increase in yield of the electron transfer products and a decrease in the rate of

reverse electron transfer if liposomes with a negative surface charge were used. This would cause expulsion of the negatively charged reduced species and a hindrance of the return of this species to the membrane surface due to Coulombic interactions. An opposite result might obtain if liposomes bearing a positive charge were employed. Since glycolipids are known to be the most abundant lipid types found in photosynthetic membranes it would also be of interest to determine what properties these lipids bestow on this photo-induced electron transfer reaction.

Other studies relevant to photosynthesis would involve using Chl dimers since these are functional in the primary electron transfer reaction of _in vivo_ photosynthesis. Incorporating Phe into the system would likewise be of interest since Phe is known to function as a primary electron acceptor _in vivo_. Increasing the complexity of the system by adding additional components such as cytochromes and other redox components would bring the system closer to the biological reality. Other processes known to occur in photosynthesis which would be amenable to investigation in the Chl-liposome system or some variation thereof, include vectorial electron transfer across the membrane, proton pumping and oxygen evolution, all of which are light-driven processes.

APPENDIX A

LIST OF SYMBOLS AND ABBREVIATIONS

$\mathring{A}$	angstrom unit
BChl	bacteriochlorophyll
BLM	bilayer lipid membrane (planar)
BPhe	bacteriopheophytin
BQ	p-benzoquinone
$BQ^{-\cdot}$	p-benzosemiquinone anion radical
CCCP	carbonylcyanide-m-chlorophenylhydrazone
Chl	chlorophyl *a*
Chl b	chlorophyll *b*
Chl-liposome	chlorophyll *a*-containing liposome
$Chl^{+\cdot}$	chlorophyll cation radical
Chl_g	chlorophyll ground state
Chl_t	chlorophyll triplet state
Chl_s	chlorophyll singlet state
cyt c	cytochrome c
DMPC	dimyristoyl phosphatidylcholine (14:0)*
DMA	N,N-dimethylaniline
DMA^{+}	cation of DMA
DOPC	dioleoyl phosphatidylcholine (18:1)*
DQ	duroquinone
DPPC	dipalmitoyl phosphatidylcholine (16:0)*
DSPC	distearoyl phosphatidylcholine (18:0)*
DTBQ	2,6-di-t-butyl-p-benzoquinone
EDTA	ethylenediamine-N,N,N',N'-tetraacetate
EPR	electron paramagnetic resonance
g	gyromagnetic ratio
G	gauss
k_q	quenching rate constant
MV^{+2}	methyl viologen
$MV^{+\cdot}$	methyl viologen radical
MW	molecular weight
NMR	nuclear magnetic resonance
OD	optical density

P_{680}	photosystem II
P_{700}	photosystem I
PC	phosphatidylcholine
Phe	pheophytin
PMT	photomultiplier tube
PS I	photosystem I
PS II	photosystem II
Q	quinone
$Q^{\cdot -}$	semiquinone anion radical
τ	lifetime
T_c	phase transition temperature
TMPD	N,N,N'N'-tetramethyl-p-phenylenediamine
UQ	ubiquinone
$UQ^{\cdot -}$	ubisemiquinone anion radical
V	voltage

* In this notation the first number represents the number of carbon atoms in the fatty acid chains of the lipid molecules while the second number represents the number of double bonds in the chain.

SELECTED BIBLIOGRAPHY

1. Feher, G., A. J. Hoff, R. A. Isaacson and L. C. Ackerson (1975) Annals N.Y. Acad. Sci. 244, 239-259.

2. Katz, J. J., W. Oettmeier and J. R. Norris (1976) Phil. Tran. R. Soc. Lond. B273, 227-253.

3. Shipman, L. L., T. M. Cotton, J. R. Norris and J. J. Katz (1976) Proc. Natl. Acad. Sci. USA 73, 1791-1794.

4. Katz, J. J., J. R. Norris, L. L. Shipman, M. C. Thurnauer and M. R. Wasielewski (1978) Ann. Rev. Biophys. Bioeng. 7, 393-434.

5. Fajer, J., D. C. Brune, M. S. Davis, A. Forman and L. D. Spaulding (1975) Proc. Natl. Acad. Sci. USA 72, 4956-4960.

6. Holten, D., W. W. Parson and J. P. Thornber (1978) Biochim. Biophys. Acta 501, 112-126.

7. Fajer, J., M. S. Davis, A. Forman, V. V. Klimov, E. Dolan and B. Ke (1980) J. Am. Chem. Soc. 102, 7143-7145.

8. Wraight, C. A. and R. K. Clayton (1973) Biochim. Biophys. Acta 333, 246-260.

9. Borisov, A. Y. and M. D. Ilina (1973) Biochim. Biophys. Acta 325, 240-246.

10. Lauger, P., G. W. Pohl, A. Steinemann and H. W. Trissl (1974) In Perspectives in Membrane Biology (Edited by S. Estrada-O and C. Gilter) pp. 645-659. Academic Press, New York.

11. Calvin, M. (1978) Acc. Chem. Res. 11, 369-374.

12. Fendler, J. H. (1980) Acc. Chem. Res. 13, 7-13.

13. Katz, J. J. and T. R. Janson (1976) Trans. Am. Nucl. Soc. 23, 106-107.

14. Proceedings of the Symposium on Photoelectric Bilayer Lipid Membranes(1976) Photochem. Photobiol. 24, 95-207.

15. Tien, H. T. (1979) In Topics in Photosynthesis, Vol. 3 (Edited by J. Barber) pp. 115-173. Elsevier Scientific Publishing Co., Amsterdam.

16. Lindig, B. A. and M. A. J. Rodgers (1980) Photochem. Photobiol. 31, 617-622.

17. Turro, N. J., M. Gratzel and A. M. Braun (1980) Angew. Chem. Int. Ed. Engl. 19, 675-696.

18. Wolff, C. and M. Gratzel (1977) Chem. Phys. Lett. 52, 542-545.

19. Yoshimura, A. and S. Kato (1980) Bull. Chem. Soc. Jpn. 53, 1877-1880.

20. Mukherjee, T., A. V. Sapre and J. P. Mittal (1978) Photochem. Photobiol. 28, 95-96.

21. Brown, R. G. and E. H. Evans (1980) Photochem. Photobiol. 32, 103-105.

22. Cheddar, G., F. Castelli and G. Tollin (1980) Photochem. Photobiol. 32, 71-78.

23. Seely, G. R. (1976) J. Phys. Chem. 80, 447-451.

24. Seely, G. R. and A. M. Rutkowski (1980) Abs. Third Int. Conf. Photochem. Conversion and Storage of Solar Energy, 109-111.

25. Costa, S. M. B. and G. Porter (1974) Proc. R. Soc. Lond. A. 341, 167-176.

26. Hirsch, R. E. and S. S. Brody (1980) Arch. Biochem. Biophys. 199, 506-514.

27. Beddard, G. S., G. Porter and G. M. Weese (1975) Proc. R. Soc. Lond. A 352, 317-325.

28. Iriyama, K. (1980) J. Membr. Biol. 52, 115-120.

29. Dodelet, J. P., M. Ringuet, M. F. Lawrence and R. M. LeBlanc (1980) Abs. Third Int. Conf. Photochem. Conversion and Storage of Solar Energy, 21-22.

30. Janzen, A. F., J. R. Bolton and M. J. Stillman (1979) J. Am. Chem. Soc. 101, 6337-6341.

31. Janzen, A. F. and J. R. Bolton (1979) J. Am. Chem. Soc. 101, 6342-6347.

32. Miyasaka, T., T. Watanabe, A. Fujishima and K. Honda (1978). J. Am. Chem. Soc. 100, 6657-6665.

33. Watanabe, T., T. Miyasaka, A. Fujishima and K. Honda (1978) Chem. Lett. 443-446.

34. Kiwi, J. and M. Gratzel (1980) J. Phys. Chem. 84, 1503-1507.

35. Jones, C. E., C. A. Jones and R. A. MacKay (1979) J. Phys. Chem. 83, 805-810.

36. Jones, C. A., L. E. Weaner and R. A. MacKay (1980) J. Phys. Chem. 84, 1495-1500.

37. Widart, M. and J. Aghion (1980) Photobiochem. Photobiophys. 1, 225-274.

38. Borg, D. C., J. Fajer, R. H. Felton and D. Dolphin (1970) Proc. Natl. Acad. Sci. USA 67, 813-820.

39. Fukuzumi, S., Y. Ono and T. Keii (1973) Bull. Chem. Soc. Jpn. 46, 3353-3355.

40. Linschitz, H. and K. Sarkanen (1958) J. Am. Chem. Soc. 80, 4826-4832.

41. Tollin, G. and G. Green (1962) Biochim. Biophys. Acta 60, 524-538.

42. Tollin, G., F. Castelli, G. Cheddar and F. Rizzuto (1979) Photochem. Photobiol. 29, 147-152.

43. Huppert, D., P. M. Rentzepis and G. Tollin (1976) Biochim. Biophys. Acta 440, 356-364.

44. Chibisov, A. K. (1969) Photochem. Photobiol. 10, 331-345.

45. White, R. A. and G. Tollin (1971) Photochem. Photobiol. 14, 43-63.

46. Cheddar, G. and G. Tollin (1980) Photobiochem. Photobiophys. 1, 235-241.

47. Harbour, J. and G. Tollin (1974) Photochem. Photobiol. 19, 147-161.

48. Mukherjee, D. C., D. H. Cho and G. Tollin (1969) Photochem. Photobiol. 9, 273-289.

49. Hales, B. J. and J. R. Bolton (1972) J. Am. Chem. Soc. 94, 3314-3320.

50. Kunitake, T., Y. Okahata, K. Tamaki, F. Kumamaru and M. Takayanagi (1977) Chem. Lett. 387-390.

51. Tran, C. D., P. L. Klahn, A. Romero and J. H. Fendler (1978) J. Am. Chem. Soc. 100, 1622-1624.

52. McNeil, R. and J. K. Thomas (1980) J. Colloid Interface Sci. 73, 522-528.

53. Tanford, C. (1980) The Hydrophobic Effect, Second Edition, Wiley, New York.

54. Bangham, A. D., M. M. Standish and J. C. Watkins (1965) J. Mol. Biol. 13, 238-252.

55. Huang, C. (1969) Biochem. 8, 344-351.

56. Batzri, S. and E. D. Korn (1973) Biochim. Biophys. Acta 298, 1015-1019.

57. Deamer, D. and A. D. Bangham (1976) Biochim. Biophys. Acta 443, 629-634.

58. Kremer, J. M. H., M. W. J. v.d. Esker, C. Pathmamanoharan and P. Wiersema (1977) Biochem. 16, 3932-3935.

59. Brunner, J., P. Skrabal and H. Hauser (1976) Biochim. Biophys. Acta 455, 322-331.

60. Barenholz, Y., D. Gibbs, B. J. Littman, J. Goll, T. E. Thompson and F. D. Carlson (1977) Biochem. 16, 2806-2810.

61. Szoka, Jr., F. and D. Papahadjopoulus (1980) In Ann. Rev. Biophys. Bioenerg. 9 (Edited by L. J. Mullins) pp. 467-508, Ann. Rev. Inc., Palo Alto, CA.

62. Chapman, D. and P. G. Fast (1968) Science 160, 188-189.

63. Stillwell, W. and H. T. Tien (1977) Biochem. Biophys. Res. Comm. 76, 232-238.

64. Stillwell, W. and H. T. Tien (1977) Biochim. Biophys. Acta 461, 239-252.

65. Ritt, E. and D. Walz (1976) J. Membr. Biol. 27, 41-54.

66. Dijkmans, H., R. M. LeBlanc, F. Cogniaux and J. Aghion (1979) Photochem. Photobiol. 29, 367-372.

67. Dijkmans, H., F. Cogniaux and J. Aghion (1979) Biochem. Biophys. Res. Comm. 89, 1141-1145.

68. Trosper, T., D. Raveed and B. Ke (1970) Biochim. Biophys. Acta 223, 463-465.

69. Oetmeier, W., J. R. Norris and J. J. Katz (1976) Biochem. Biophys. Res. Comm. 71, 445-451.

70. Luisetti, J., H. Hohwald and H. J. Galla (1977) Biochem. Biophys. Res. Comm. 78, 754-760.

71. Fragata, M. (1977) Experientia 33, 177-179.

72. Steinemann, A., N. Alamuti, W. Brodman, O. Marshall and P. Lauger (1971) Membr. Biol. 4, 284-294.

73. Cherry, R. J., K. Hsu and D. Chapman (1972) Biochim. Biophys. Acta 267, 512-522.

74. Cherry, R. J., K. Hsu and D. Chapman (1971) Biochem. Biophys. Res. Comm. 43, 351-358.

75. Steinemann, A., G. Stark and P. Lauger (1972) J. Membr. Biol. 9, 177-194.

76. Weller, H. G. and H. T. Tien (1973) Biochim. Biophys. Acta 325, 433-440.

77. Hoff, A. J. (1974) Photochem. Photobiol. 19, 51-57.

78. Podo, F., J. E. Cain, J. K. Blaisie (1976) Biochim. Biophys. Acta 419, 19-41.

79. Lee, A. G. (1975) Biochem. 14, 4397-4402.

80. Walz, D. (1976) J. Membr. Biol. 27, 55-81.

81. Walz, D (1977) J. Membr. Biol. 31, 31-64.

82. Livingston, R. (1950) Q. Reviews Chem. Soc. 14, 174-199.

83. Lavorel, J. (1957) J. Phys. Chem. 61, 1600-1605.

84. Brody, S. S. and M. Brody (1961) Nature 189, 547-549.

85. Sauer, K. (1975) In Bioenergetics of Photosynthesis (Edited by Govindgee) pp. 131-136, Academic Press, New York.

86. Beddard, G. S. and G. Porter (1976) Nature 260, 366-369.

87. Katz, J. J., J. R. Norris and L. L. Shipman (1977) Brookhaven Symposia in Biology, 28, 16-55.

88. Yuen, M. J., L. L. Shipman, J. J. Katz and J. C. Hindman (1980) Photochem. Photobiol. 32, 281-296.

89. Colbow, K. (1973) Biochim. Biophys. Acta 318, 4-9.

90. Lee, A. G. (1975) Biochim. Biophys. Acta 413, 11-23.

91. Nicholls, P., J. West and A. D. Bangham (1974) Biochim. Biophys. Acta 363, 190-201.

92. Knoll, W., J. Bauman, P. Korpium and U. Theilen (1980) Biochem. Biophys. Res. Comm. 96, 968-974.

93. Luisetti, J., H. J. Galla and H. Mohwald (1978) Ber. Bunsenges. Phys. Chem. 82, 911-916.

94. Mangel, M. (1976) Biochim. Biophys. Acta 430, 459-466.

95. Brody, S. S. (1980) Photobiochem. Photobiophys. 1, 289-295.

96. Beddard, G. S., S. B. Carlin and G. Porter (1976) Chem. Phys. Lett. 43, 27-32.

97. Fragata, M. (1978) J. Colloid Interface Sci. 66, 470-474.

98. Tomkiewicz, M. and G. Corker (1974) In Proceedings of the Third International Congress on Photosynthesis (Edited by M. Avron) pp. 265-272. Elsevier Scientific Publishing Co., Amsterdam, The Netherlands.

99. Tomkiewicz, M. and G. Corker (1975) Photochem. Photobiol. 22, 249-256.

100. Borg, D. C., J. Fajer, R. H. Felton and D. Dolphin (1970) Proc. Natl. Acad. Sci. USA 67, 813-820.

101. Oettmeier, W., J. R. Norris and J. J. Katz (1976) Z. Naturforsch. 31c, 163-168.

102. Kurihara, K., M. Sukigara and Y. Toyoshima (1979) Biochim. Biophys. Acta 547, 117-126.

103. Kurihara, K., Y. Toyoshima and M. Sukigara (1979) Biochem. Biophys. Res. Comm. 88, 320-326.

104. Toyoshima, Y., M. Morino, H. Motoki and M. Sukigara (1977) Nature 265, 187-189.

105. Stillwell, W. and H. T. Tien (1978) Biochem. Biophys. Res. Comm. 81, 212-216.

106. Strain, H. H. and W. A. Svec (1966) In The Chlorophylls (Edited by L. P. Vernon) pp. 22-66. Academic Press, New York.

107. Wells, M. A. and D. J. Hanahan (1969) In Methods in Enzymology (Edited by J. M. Lowenstein) Vol. XIV, pp. 179-181. Academic Press, New York.

108. Yabusaki, K. K. (1975) Ph.D. Dissertation, University of Arizona.

109. D'Anna Jr., J. A. and G. Tollin (1971) Biochem. 10, 57-64.

110. Castelli, F. (1976) Chem. Phys. Lett. 38, 528-531.

111. Seely, G. R. and R. G. Jensen (1965) Spectrochim. Acta 21, 1835-1845.

112. Huang, C. and J. L. Mason (1978) Proc. Natl. Acad. Sci. USA 75, 308-310.

113. Bruce, J. M. (1974) In The Chemistry of the Quinoid Compounds (Edited by S. Patai) pp. 465-538. John Wiley and Sons, London.

114. Kuboyama, A., R. Yamazaki, S. Yabe and Y. Uehara (1969) Bull. Chem. Soc. Jpn. 42, 10-15.

115. Scatchard, G. (1949) Ann. N.Y. Acad. Sci. 51, 660-672.

116. Huang, C. and J. P. Charlton (1972) Biochem. 11, 735-740.

117. Fukushima, D., S. Yokoyama, D. J. Kroon, F. J. Kezdy and E. T. Kaiser, J. Biol. Chem. 255, 10651-10657.

118. Poupe, F. (1947) Coll. Czech. Chem. Comm. 12, 225-236.

119. Weber, G. and F. W. J. Teale (1957) Trans. Faraday Society 53, 646-655.

120. Bowers, P. G. and G. Porter (1967) Proc. R. Soc. London A296, 435-441.

121. Pileni, M. P., A. M. Braun and M. Gratzel (1980) Photochem. Photobiol. 31, 423-427.

122. Turro, N. J., K. C. Lin, M. F. Chow and P. Lee (1978) Photochem. Photobiol. 27, 523-528.

123. Humphry-Baker, R., Y. Moroi and M. Gratzel (1978) Chem. Phys. Lett. 58, 207-210.

124. Kalyanasundaram, K., F. Grieser and J. K. Thomas (1977) Chem. Phys. Lett. 51, 501-505.

125. Pileni, M. P. (1980) Chem. Phys. Lett. 71, 317-321.

126. Maestri, M., P. Infelta and M. Gratzel (1978) J. Chem. Phys. 69, 1522-1526.

127. McConnell, H. M., P. Devaux and C. Scandella (1972) In Membrane Research (Edited by C. F. Fox) pp. 27-37. Academic Press, New York.

128. Lee, A. G., N. J. M. Birdsall and J. C. Metcalfe (1973) Biochem. 12, 1650-1659.

129. Cogan, U., M. Shinitzky, G. Weber and T. Nishida (1973) Biochem. 12, 521-528.

130. Shinitzky, M. and Y. Barenholz (1974) J. Biol. Chem. 249, 2652-2657.

131. Frost, A. A. and R. G. Pearson (1963) Kinetics and Mechanism p. 271. Wiley, New York.

132. Ladbrooke, B. D. and D. Chapman (1969) Chem. Phys. Lipids 3, 304-319.

133. Tollin, G. (1976) J. Phys. Chem. 80, 2274-2277.

134. Gouterman, M. and D. Holten (1977) Photochem. Photobiol. 25, 85-92.

135. Chibisov, A. K. (1969) Photochem. Photobiol. 10, 331-347.

136. Peover, M. D. (1962) J. Chem. Soc., 4540-4549.

137. Marcus, M. F. and M. D. Hawley (1971) Biochim. Biophys. Acta 226, 234-238.

138. Shah, S. S., D. Holten and M. W. Windsor (1980) Photobiochem. Photobiophys. 1, 361-373.

139. Franck, J. and E. Rabinowitch (1934) Trans. Faraday Soc. 30, 120-131.

140. Noyes, R. M. (1960) Z. Electrochem. 64, 153-156.

141. Nagamura, T., K. Takama, Y. Tsutsui and T. Matsuo (1980) Chem. Lett., 503-506.

142. Moroi, Y., A. M. Braun and M. Gratzel (1979) J. Am. Chem. Soc. 101, 567-572.

143. Gratzel, M. (1979) Isr. J. Chem. 18, 364-368.

144. Layloff, T., T. Miller, R. N. Adams, H. Fah, A. Horsfield and W. Proctor (1965) Nature 205, 382-383.

145. Miller, T. A. and R. N. Adams (1966) J. Am. Chem. Soc. 88, 5713-5714.

146. deBoer, E. and H. van Willigen (1967) In Prog. Nucl. Mag. Reson. Spect. (Edited by J. W. Emsley, J. Feeney and L. H. Sutcliffe) Vol. 2, pp. 111-161. Pergamon Press, Oxford.

147. Meisel, D. and R. W. Fessenden (1976) J. Am. Chem. Soc. 98, 7505-7510.

148. Hauska, G. (1977) In Bioenergetics of Membranes (Edited by L. Packer, G. C. Papageorgiou and A. Trebst) pp. 177-187. Elsevier/North Holland Biomedical Press, Amsterdam.

149. Vermeglio, A. and R. K. Clayton (1977) Biochim. Biophys. Acta 461, 159-165.